

Dense heteroclinic tangencies near a Bykov cycle

Isabel S. Labouriau Alexandre A. P. Rodrigues
 Centro de Matemática da Universidade do Porto *
 and Faculdade de Ciências, Universidade do Porto
 Rua do Campo Alegre, 687, 4169-007 Porto, Portugal
 islabour@fc.up.pt alexandre.rodrigues@fc.up.pt

Keywords

Heteroclinic cycle, heteroclinic tangencies, non-hyperbolicity, strange attractors, spiralling sets

2010 — AMS Subject Classifications

Primary: 34C28

Secondary: 34C37, 37C29, 37D05, 37G35

Abstract

This article presents a mechanism for the coexistence of hyperbolic and non-hyperbolic dynamics arising in a neighbourhood of a Bykov cycle where trajectories turn in opposite directions near the two nodes — we say that the nodes have different chirality. We show that in a C^2 -open class of vector fields defined on a three-dimensional compact manifold, tangencies of the invariant manifolds of two hyperbolic saddle-foci occur at a full Lebesgue measure set of the parameters that determine the linear part of the vector field at the equilibria. This has important consequences: the global dynamics is persistently dominated by heteroclinic tangencies and by Newhouse phenomena, coexisting with hyperbolic dynamics arising from transversality. The coexistence gives rise to linked suspensions of Cantor sets, with hyperbolic and non-hyperbolic dynamics, in contrast with the case where the nodes have the same chirality.

We illustrate our theory with an explicit example where tangencies arise in the unfolding of a symmetric vector field on the three-dimensional sphere.

1 Introduction

Heteroclinic cycles and networks are flow-invariant sets that occur in a robust way in the flow of equivariant differential equations, and are known to provide a mechanism for intermittent behaviour in these systems. Heteroclinic dynamics appears in models for a wide range of phenomena including economics and game theory [1], bursting of neurones [10], cryptography [36] and the geomagnetic field [31, 38]. Heteroclinic cycles may be considered as the skeleton for understanding complicated switching between physical states; although a heteroclinic cycle has simple dynamics, it may induce subtle and complex behaviour around it.

Structurally stable heteroclinic cycles in symmetric systems have been studied by several authors, since the canonical example presented by Guckenheimer and Holmes [20]. The dynamics near a heteroclinic cycle is characterised by intermittency: a solution that remains near the cycle spends a long time close to each node and makes fast transitions from one node to the next. If the cycle is attracting, then as nearby solutions approach it, the time spent near each equilibrium increases geometrically. Conditions for the existence and stability of heteroclinic cycles in systems with symmetry have been derived by Krupa and Melbourne [25, 26].

*CMUP is supported by the European Regional Development Fund through the programme COMPETE and by the Portuguese Government through the Fundação para a Ciência e a Tecnologia (FCT) under the project PEst-C/MAT/UI0144/2011. A.A.P. Rodrigues was supported by the grants SFRH/BD/28936/2006 and SFRH/BPD/84709/2012 of FCT.

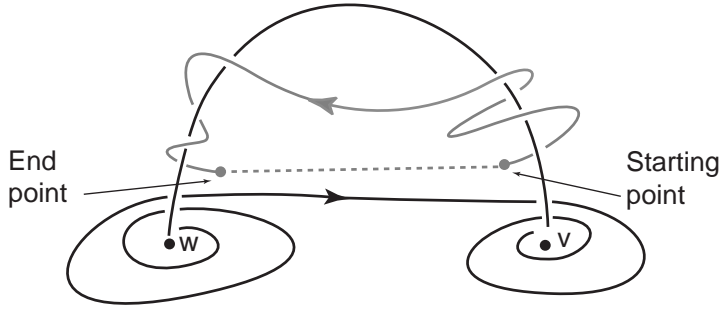


Figure 1: Bykov cycle with saddle-foci of different chirality. The starting point of a nearby trajectory is joined to its end point forming a loop. Arbitrarily close to the cycle there are trajectories whose loop is not linked to the cycle. This happens because near each saddle-focus trajectories turn around the one-dimensional connection in opposite directions.

A good deal about bifurcations of heteroclinic cycles and networks is now known — see for instance [2, 13, 30]. Some results about the effect of symmetry-breaking on the dynamics have been obtained in [24, 27, 40, 41]. The rigorous analysis of the intermittent dynamics associated to the structure of the nonwandering sets close to heteroclinic networks is still a challenge. We refer to Homburg and Sandstede [22] for an overview of heteroclinic bifurcation and for details on the dynamics near different kinds of heteroclinic cycles and networks.

A persistent attractor with complex geometry occurs near heteroclinic cycles where each node is either a saddle-focus or a non-trivial periodic solution. Due to the rotation around the saddles, the non-wandering set associated to the cycle has a spiral structure as predicted by Arneodo *et al* [5]. The complex geometry of this spiralling set is probably the reason why this subject was left almost untouched from L. P. Shilnikov [43] to P. Holmes [21].

An example of a heteroclinic network involving several hyperbolic equilibria, where trajectories switch around the different cycles of the network, is described by Aguiar *et al* [2]. A symmetry reduction argument yields a quotient network with two saddle-foci of different Morse indices reminiscent of those studied by Bykov [9]. Under the assumption that near the two equilibria trajectories wind in the same direction around the one-dimensional heteroclinic connection, it may be shown that each small tubular neighbourhood of the network contains suspended horseshoes [2, 27]. In this case, some of the connections in the network arise from transverse intersections of stable and unstable manifolds of equilibria. Rodrigues [39] has proved that Lebesgue almost all solutions do not remain near the cycle for all time, although they may return to the cycle after an excursion away from it.

In the context of heteroclinic cycles with two saddle-foci, there are two different possibilities for the geometry of the flow around the cycle, depending on the direction trajectories turn around the heteroclinic connection of one-dimensional invariant manifolds — see Figure 1. In [2, 4, 27, 28, 40], the authors assumed, sometimes implicitly, that in the neighbourhood of the two saddle-foci trajectories wind in the same direction around a heteroclinic connection of one-dimensional invariant manifolds — the two nodes have *the same chirality*. A natural question arises: what is the dynamics near a Bykov cycle whose nodes do not have the same chirality?

In the case of reversible equations where the anti-symmetry is a reflection, if the two nodes have different chirality, then the rotations may cancel out. To the best of our knowledge neither this situation, nor the general non-reversible case have been rigorously studied. Here, we show that the orientation of the flow around the one-dimensional manifolds has profound effects on the dynamics near the cycle; moreover, we show that different chirality may imply lack of uniform hyperbolicity near the cycle.

In the case of different chirality, we find an open condition under which the flow exhibits heteroclinic tangencies — non-transverse intersections of the stable and unstable manifolds of hyperbolic saddles. Such tangencies have been recognised as a mechanism for instability and lack of hyperbolicity in surface diffeomorphisms. One of the first results in this direction was established by Gavrilov and Shilnikov [15] for two-dimensional maps. To understand this phenomenon it is important to study the variety of dynamical behaviour associated to the creation and destruction of tangencies.

Tangencies of invariant manifolds are associated to Newhouse phenomena: bifurcations leading to the birth of infinitely many asymptotically stable periodic solutions [33, 34]. This is important for applications, since heteroclinic tangencies are ubiquitous in strange attractors. Although periodic attractors arising from tangencies have quite large periods and small basins of attraction, an infinite number of them may change the character of the chaotic dynamics.

Our work also forms part of a program, started by Bykov [9], addressing the systematic study of the dynamics near networks of equilibria whose linearisation has a conjugate pair of non real eigenvalues – this is what we call a *rotating node*. The analysis uses a classical approach of composition of Poincaré maps. Under an open condition on the parameters, we find a dense set of parameters where we prove that hyperbolic horseshoes coexist with a non-hyperbolic set with heteroclinic tangencies that cannot be separated from the hyperbolic horseshoes. Although each individual tangency may be eliminated by a small perturbation, another tangency is created nearby. Our study can be useful to locate cocoon bifurcations near a Bykov cycle, a phenomenon observed by Lau in the Michelson system — details in [11].

Structure of the article: We study the set of non-wandering points near a Bykov cycle in \mathbf{S}^3 and show the existence of heteroclinic tangencies. In Section 2, after recalling some preliminary definitions, we state the main results, Theorems 1 and 2. Their dynamical consequences are discussed in Section 3. We establish the notation and framework for the proof of Theorem 1 in Section 4 where we linearise the vector field around each equilibrium obtaining a geometrical description of the way the flow transforms a curve of initial conditions lying across the stable manifold of an equilibrium. Section 5 contains more precise statements of Theorems 1 and 2 and their proofs. This is followed in Section 6 by an example of a symmetric vector field with these properties, illustrated by numerical simulations.

2 Description of the problem

2.1 Preliminaries

Let f be a smooth vector field defined on a 3-dimensional smooth manifold. Given two equilibria p and q of $\dot{x} = f(x)$, a *heteroclinic connection* from p to q , denoted $[p \rightarrow q]$, is a flow-invariant subset of $W^u(p) \cap W^s(q)$. In this article we consider mostly 1-dimensional, sometimes 2-dimensional, connections between equilibria. We are interested in *heteroclinic cycles* associated to two hyperbolic equilibria p and q : the set consisting of the equilibria and two heteroclinic connections $[p \rightarrow q], [q \rightarrow p]$. Sometimes we refer to the equilibria on the cycle as *nodes*. More general information may be found in [6, 12].

The dimension of the unstable manifold of a hyperbolic equilibrium is called the *Morse index* of the equilibrium. A saddle-focus p is an equilibrium of $\dot{x} = f(x)$ whose spectrum $df(p)$ has two complex non-real eigenvalues $\alpha \pm i\omega$ and one real eigenvalue β with $\alpha\beta < 0$. A *Bykov cycle* is a heteroclinic cycle associated to two hyperbolic saddle-foci with different Morse indices, in which the one-dimensional invariant manifolds coincide and the two-dimensional invariant manifolds have a transverse intersection. The presence of the two connections in a Bykov cycle implies the existence of infinitely many subsidiary connections following the original cycle – see Labouriau and Rodrigues [27].

2.2 Hypothesis

Our object of study is the dynamics around a special type of Bykov cycle, for which we give a rigorous description here. Specifically, we study a C^2 -vector field f on a manifold diffeomorphic to the three-sphere $\mathbf{S}^3 = \{X = (x_1, x_2, x_3, x_4) \in \mathbf{R}^4 : \|X\| = 1\}$ whose flow has the following properties (see Figure 2):

(P1) There are two hyperbolic saddle-foci \mathbf{v} and \mathbf{w} . The eigenvalues of df_X are:

- (a) $-C_{\mathbf{v}} \pm \alpha_{\mathbf{v}}i$ and $E_{\mathbf{v}}$ where $C_{\mathbf{v}}$, $E_{\mathbf{v}}$ and $\alpha_{\mathbf{v}}$ are positive, for $X = \mathbf{v}$;
- (b) $E_{\mathbf{w}} \pm \alpha_{\mathbf{w}}i$ and $-C_{\mathbf{w}}$ where $C_{\mathbf{w}}$, $E_{\mathbf{w}}$ and $\alpha_{\mathbf{w}}$ are positive, for $X = \mathbf{w}$.

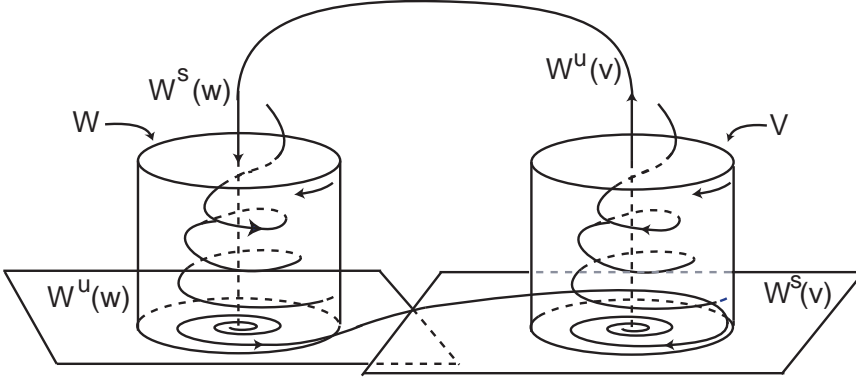


Figure 2: Geometry near a Bykov cycle with saddle-foci of different chirality. A trajectory starting in a neighbourhood V of \mathbf{v} turns around the connection $[\mathbf{v} \rightarrow \mathbf{w}]$ in one direction. After the trajectory arrives at a neighbourhood W of \mathbf{w} it turns around $[\mathbf{v} \rightarrow \mathbf{w}]$ in the opposite direction.

(P2) There is a heteroclinic cycle Γ consisting of \mathbf{v} , \mathbf{w} and two one-dimensional heteroclinic connections $[\mathbf{v} \rightarrow \mathbf{w}]$ and $[\mathbf{w} \rightarrow \mathbf{v}]$.

(P3) At the heteroclinic connection $[\mathbf{w} \rightarrow \mathbf{v}]$, the two-dimensional manifolds $W^u(\mathbf{w})$ and $W^s(\mathbf{v})$ meet transversely.

There are two different possibilities for the geometry of the flow around Γ , depending on the direction trajectories turn around the heteroclinic connection $[\mathbf{v} \rightarrow \mathbf{w}]$. To make this rigorous, we need some new concepts. Let V and W be small disjoint neighbourhoods of \mathbf{v} and \mathbf{w} with disjoint boundaries ∂V and ∂W , respectively. Trajectories starting at ∂V near $W^s(\mathbf{v})$ go into the interior of V in positive time, then follow the connection $[\mathbf{v} \rightarrow \mathbf{w}]$, go inside W , and then come out at ∂W as in Figure 2. Let φ be a piece of trajectory like this from ∂V to ∂W . Now join its starting point to its end point by a line segment as in Figure 1, forming a closed curve, that we call the *loop* of φ . For generic starting points, the loop of φ and the cycle Γ are disjoint closed curves. We say that the two saddle-foci \mathbf{v} and \mathbf{w} in Γ have the same *chirality* if the loop of every trajectory is linked to Γ in the sense that the two closed curves cannot be disconnected by an isotopy. Otherwise, we say that \mathbf{v} and \mathbf{w} have different chirality: given the neighbourhoods V and W , it is always possible to find a trajectory φ going through V and W whose loop is not linked to Γ . Then our assumption is:

(P4) The saddle-foci \mathbf{v} and \mathbf{w} have different chirality.

The transverse intersection of $W^u(\mathbf{w})$ and $W^s(\mathbf{v})$ of (P3) persists under C^1 -perturbations, whereas the connection $[\mathbf{v} \rightarrow \mathbf{w}]$ does not, unless there is some special property, like symmetry.

Property (P4) is persistent under isotopies: if it holds for f , then it is still valid in continuous (not necessarily smooth) one-parameter families containing it, as long as there is still a connection. This is particularly important when we consider unfoldings of f .

2.3 Statement of the main results

The main result in this article guarantees that heteroclinic tangencies are generic in a class of systems with Bykov cycles with different chirality. We prove that these tangencies occur in a full Lebesgue measure set in the parameters that determine the linear part of the vector field at the equilibria. They lie near the cycle, in contrast to the findings of [27, 28, 40], for cycles with the same chirality, where tangencies appear far from the heteroclinic cycle.

Given two disjoint neighbourhoods V of \mathbf{v} and W of \mathbf{w} with disjoint boundaries, ∂V and ∂W , respectively, consider a point in $[\mathbf{v} \rightarrow \mathbf{w}] \cap \partial V$ and a neighbourhood in ∂V of this point that is also

a cross-section to f . Saturating the cross-section by the flow, one obtains a flow-invariant tube joining V to W and containing the connection in its interior. A similar flow-invariant tube may be obtained around the connection $[\mathbf{w} \rightarrow \mathbf{v}]$ joining W to V . We call the union of V and W with these tubes, a *tubular neighbourhood* of the Bykov cycle.

The next results hold for vector fields in \mathbf{S}^3 under the C^k topology, for $k \geq 2$.

Theorem 1 *There is an open set \mathcal{C} of vector fields satisfying (P1)–(P4) such that for any $f \in \mathcal{C}$, and any tubular neighbourhood U of the Bykov cycle, there are vector fields on \mathbf{S}^3 arbitrarily close to f , with a Bykov cycle in U with the same properties, for which $W^u(\mathbf{w})$ and $W^s(\mathbf{v})$ have a tangency inside U .*

A more precise statement of this result will be given in Section 5. The open set \mathcal{C} corresponds to an open condition on the eigenvalues of the linearisation of the vector field that, by Thom’s Transversality Theorem, defines an open set in the C^2 topology. The set of vector fields with a heteroclinic tangency is dense in \mathcal{C} and corresponds to a subset of eigenvalues with full Lebesgue measure.

Definition 1 *Let W be a small neighbourhood of \mathbf{w} and let $\Sigma \subset W$ be a cross-section to the flow meeting $W^u(\mathbf{w})$. A one-dimensional connection $[\mathbf{w} \rightarrow \mathbf{v}]$ that meets Σ at precisely $n \in \mathbf{N}$ points is called a n -pulse heteroclinic connection $[\mathbf{w} \rightarrow \mathbf{v}]$ with respect to Σ .*

The tangencies of invariant manifolds coexist with transverse intersections, giving rise to a hyperbolic structure similar to that obtained when (P4) does not hold as in [2, 27].

Theorem 2 *There is an open set \mathcal{E} of vector fields in \mathbf{S}^3 satisfying (P1)–(P4) for which any tubular neighbourhood U of the Bykov cycle Γ contains the following:*

1. *trajectories in $U \setminus \Gamma$ that remain in U for all time;*
2. *at least one n -pulse heteroclinic connection $[\mathbf{w} \rightarrow \mathbf{v}]$ for each $n \in \mathbf{N}$;*
3. *a cross-section $S \subset U$ containing a set of points such that at these points the dynamics of the first return to S is uniformly hyperbolic and conjugate to a full shift over a finite number of symbols. This set accumulates on the cycle.*

Moreover, the set \mathcal{E} meets the set \mathcal{C} of Theorem 1 on a non-empty open set of vector fields.

Corollary 3 *For vector fields satisfying (P1)–(P4) and in a dense subset of the open set $\mathcal{E} \cap \mathcal{C}$ tangencies of the two-dimensional invariant manifolds of the saddle-foci coexist with transverse intersections.*

3 Dynamical Consequences

We will show that transverse and tangent heteroclinic connections of two-dimensional invariant manifolds coexist near a Bykov cycle with nodes of different chirality. In this section we explore the consequences of this result.

Our analysis has been restricted to \mathbf{S}^3 , the lowest possible phase space dimension in which Bykov cycles may occur. Extension to higher dimensions may be possible using the heteroclinic centre manifold theorem, Lin’s method and similar techniques; in this article we have not attempted to do so.

3.1 Chirality

The conclusions of Theorem 2 do not depend on chirality and are the same as those for Bykov cycles of the same chirality in [2, 27, 28]: any tubular neighbourhood of the cycle contains trajectories that remain on it for all time forming infinitely many suspended horseshoes.

The main difference due to property (P4) is that any neighbourhood of a Bykov cycle with different chirality contains nontrivial and irremovable subsets with hyperbolic dynamics but it is not exhausted by them. The non-hyperbolicity takes place everywhere.

Corollary 4 *There is an open set \mathcal{C} of vector fields satisfying (P1)–(P4) such that arbitrarily close to any $f \in \mathcal{C}$, there is a vector field on \mathbf{S}^3 with a Bykov cycle with the same properties, where the non-uniformly hyperbolic dynamics cannot be separated by an isotopy from the maximal hyperbolic set that appears in any tubular neighbourhood of the cycle.*

Equations with symmetry having cycles of the same chirality may also exhibit tangencies of invariant manifolds, but they arise far from the Bykov cycle, see Labouriau and Rodrigues [28].

3.2 Tangency

In the context of dissipative diffeomorphisms containing homoclinic points, Newhouse [33, 34] introduced the term *strange attractor* for non-uniformly hyperbolic sets whose invariant manifolds have a tangency. He reported what happens in a one-parameter unfolding, when a homoclinic tangency splits, and discovered nontrivial, transitive and hyperbolic sets whose stable and unstable invariant manifolds have an irremovable nondegenerate tangency – although the tangency is removed by a small perturbation of the system, one cannot avoid the appearance of new tangencies. Fat hyperbolic sets, in the sense of Bowen [7, 8], exist for diffeomorphisms C^2 -close to any diffeomorphism with a homoclinic tangency — see Palis and Takens [37, Chapter 4]. The open regions where diffeomorphisms with homoclinic tangencies are dense are called *Newhouse regions*. Newhouse’s results on homoclinic tangencies may be adapted to the case studied here, ensuring the multiplicity of nearby stable solutions.

Corollary 5 *Let f_λ be a one-parameter family of vector fields in the open set \mathcal{C} of Theorem 1 and suppose in addition that $C_v > E_v$ and $C_w > E_w$. Then there are period doubling sequences for the first return map to any cross section to the Bykov cycle. Moreover, there are persistent heteroclinic tangencies of the invariant manifolds of periodic solutions and infinitely many periodic sinks nearby.*

Proof: This follows from results by Mora and Viana [32], Palis and Takens [37] and Yorke and Alligood [47], to which the reader is also referred for more details on the bifurcation sequences giving rise to these dynamical properties. \square

Near a heteroclinic tangency there is no dominated splitting of the tangent space into stable and unstable subspaces. In the C^1 -topology, the existence of tangencies and the absence of dominated splittings are synonymous — see Wen [46].

In the conservative and reversible settings, it is known that there are coexisting Newhouse regions in which a dense set of maps possess simultaneously infinitely many asymptotically stable, saddle, completely unstable and elliptic periodic orbits — see [29] and references therein.

The description of the set of all solutions that lie near a non-transverse intersection of invariant manifold becomes complicated. As reported in Gonchenko *et al* [18], the main source of the difficulty is that arbitrarily small perturbations of any system with the simplest tangency may lead to the creation of new tangencies of arbitrarily high orders, and to the birth of periodic trajectories of arbitrarily high orders of degeneracy.

3.3 The spiralling set

A transverse intersection of two-dimensional invariant manifolds $W^u(\mathbf{w})$ and $W^s(\mathbf{v})$ cannot be removed by a small smooth perturbation. Near it the set of all solutions that never leave a neighbourhood of the heteroclinic cycle has a non-trivial structure as in Shilnikov [44]: it defines a locally maximal non-trivial hyperbolic set, and admits a complete description in terms of symbolic dynamics. When the non transverse one-dimensional connection is broken, for instance by forced symmetry-breaking as in [27], finitely many of these horseshoes persist but their number may be arbitrarily large.

The existence of hyperbolic horseshoes near the cycle gives some information about the topological entropy of the first return map [23]. Although, near the horseshoes, there are irremovable sinks with zero topological entropy, we may still conclude that:

Corollary 6 *For f in the open set \mathcal{C} of Theorem 1, the topological entropy associated to the first return map restricted to a cross section Σ to the Bykov cycle is positive.*

This means that there are trajectories with one positive Lyapunov exponent. In the presence of sectional dissipation, as in Corollary 5 we also expect the existence of a negative Lyapunov exponent.

The global attractor also contains innitely many sinks with long periods and narrow basins of attraction, arising from the heteroclinic tangencies described in Theorem 1. The maximal transitive set surrounds attracting periodic solutions that accumulate on the original cycle and coexist with hyperbolic horseshoes. The properties of the attractor are similar to the quasi-stochastic attractors studied by Gonchenko et al [17].

Homoclinic tangencies of arbitrary orders are considered by Gonchenko and Li [16] together with sufficient conditions for the existence of nontrivial hyperbolic sets containing infinitely many hyperbolic horseshoes. Their proof uses symbolic dynamics and refers to arguments of Katok [23].

4 Local Dynamics near each saddle-focus

We follow the standard procedure for modelling the dynamics near a heteroclinic network. We construct return maps defined on various cross-sections and analyse the dynamics by composing them in an appropriate order to obtain Poincaré maps modelling the dynamics near the Bykov cycle.

In this section, we establish local coordinates near the saddle-foci \mathbf{v} and \mathbf{w} and define some notation that will be used in the rest of the paper. The starting point is an application of Samovol's Theorem [42] to linearise the flow around the equilibria and to introduce cylindrical coordinates around each saddle-focus. These are used to define neighbourhoods whose boundaries are transverse to the linearised flow. For each saddle, we obtain the expression of the local map that sends points in the boundary where the flow goes in, into points in the boundary where the flows goes out. Finally, we establish a convention for the transition maps from one neighbourhood to the other. When we refer to the stable/unstable manifold of an equilibrium point, we mean the *local* stable/unstable manifold of that equilibrium.

4.1 Linearisation near the saddle-foci

By Samovol's Theorem [42], around the saddle-foci, the vector field f is C^1 -conjugate to its linear part, since there are no resonances of order 1. In cylindrical coordinates (ρ, θ, z) the linearisations at \mathbf{v} and \mathbf{w} take the form, respectively:

$$\begin{cases} \dot{\rho} = -C_{\mathbf{v}}\rho \\ \dot{\theta} = \alpha_{\mathbf{v}} \\ \dot{z} = E_{\mathbf{v}}z \end{cases} \quad \begin{cases} \dot{\rho} = E_{\mathbf{w}}\rho \\ \dot{\theta} = -\alpha_{\mathbf{w}} \\ \dot{z} = -C_{\mathbf{w}}z. \end{cases} \quad (4.1)$$

We consider cylindrical neighbourhoods of \mathbf{v} and \mathbf{w} in \mathbf{S}^3 of radius $\varepsilon > 0$ and height 2ε that we denote by V and W , respectively. Their boundaries consist of three components (see Figure 3):

- The cylinder wall parametrised by $x \in \mathbf{R} \pmod{2\pi}$ and $|y| \leq \varepsilon$ with the usual cover:

$$(x, y) \mapsto (\varepsilon, x, y) = (\rho, \theta, z).$$

Here y represents the height of the cylinder and x is the angular coordinate, measured from the point $x = 0$ in the connection $[\mathbf{w} \rightarrow \mathbf{v}]$.

- Two disks, the top and the bottom of the cylinder. We assume the connection $[\mathbf{v} \rightarrow \mathbf{w}]$ goes from the top of one cylinder to the top of the other, and we take a polar covering of the top disk:

$$(r, \varphi) \mapsto (r, \varphi, \varepsilon) = (\rho, \theta, z)$$

where $0 \leq r \leq \varepsilon$ and $\varphi \in \mathbf{R} \pmod{2\pi}$.

On these cross sections, we define the return maps to study the dynamics near the cycle.

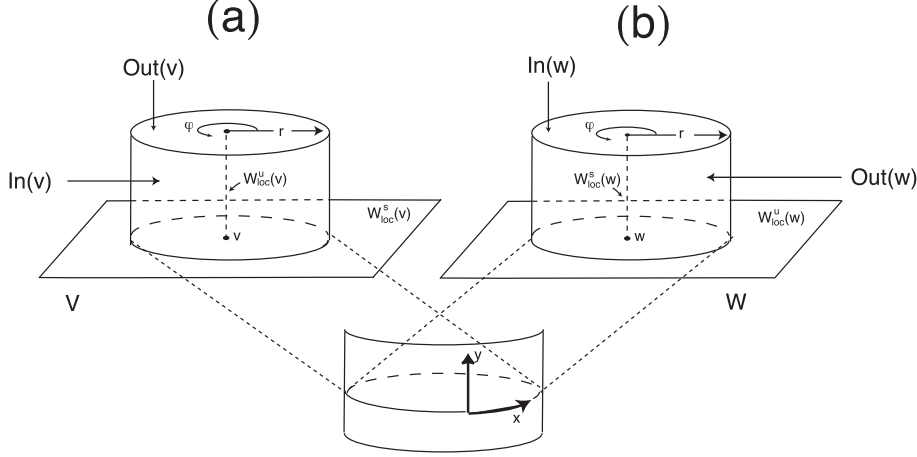


Figure 3: Parametrisation of the cylindrical neighbourhoods of the saddle-foci. (a) The flow goes into the cylinder V transversely across the wall $In(v) \setminus W^s(v)$ and leaves it transversely across its top $Out(v)$. (b) The flow goes into the cylinder W transversely across its top $In(w) \setminus W^s(w)$ and leaves it transversely across the wall $Out(w)$. Inside both cylinders, the vector field is linear. Cylinder tops are parametrised in polar coordinates (r, φ) , cylinder walls in coordinates (x, y) , with angular coordinate x .

4.2 Coordinates near v and w

Consider the cylinder wall near v , that meets $W^s(v)$ on the circle parametrised by $y = 0$. The top part $y \geq 0$ of the cylinder wall near v is denoted by $In(v)$. Trajectories starting at interior points of $In(v)$ go into the cylinder in positive time and come out at the cylinder top, denoted $Out(v)$. Trajectories starting at interior points of $Out(v)$ go inside the cylinder in negative time. After linearisation, in these coordinates, the manifold $W^u(v)$ is the z -axis, intersecting $Out(v)$ at the origin of coordinates.

Reversing the time, we get dual results for w . After linearisation, $W^s(w)$ is the z -axis, intersecting the top, $In(w)$, of the cylinder at the origin of its coordinates. Trajectories starting at interior points of $In(w)$ go into W in positive time.

Trajectories starting at interior points of the cylinder wall $Out(w)$ go into W in negative time. The set $Out(w) \cap W^u(w)$ is parametrised by $y = 0$. Trajectories that start at $In(w) \setminus W^s(w)$ leave the cylindrical neighbourhood W at $Out(w)$.

4.3 Transition Maps

In the rest of this paper, we study the Poincaré first return map on the boundaries defined above. Consider the transition maps

$$\Psi_{v,w} : Out(v) \longrightarrow In(w) \quad \text{and} \quad \Psi_{w,v} : Out(w) \longrightarrow In(v).$$

The map $\Psi_{w,v}$ can be seen as a rotation by an angle α . We use $\alpha \equiv \frac{\pi}{2}$, that simplifies the expressions used.

As in Bykov [9] and Homburg and Sandstede [22], after a rotation and a uniform rescaling of the coordinates, we may assume without loss of generality that $\Psi_{v,w}$ is the linear map $\Psi_{v,w}(x, y) = (ax, y/a)$ with $a \geq 1$.

4.4 Local maps near v and w

The flow is transverse to the above cross sections and moreover the boundaries of V and of W may be written as the closures of the disjoint unions $In(v) \cup Out(v)$ and $In(w) \cup Out(w)$, respectively. The trajectory of the point (x, y) in $In(v) \setminus W^s(v)$ leaves V at $Out(v)$ at:

$$\Phi_v(x, y) = (c_1 y^{\delta_v}, -g_v \ln y + x + c_2) = (r, \varphi) ,$$

where $\delta_{\mathbf{v}}$ is the *saddle index* of \mathbf{v} ,

$$\delta_{\mathbf{v}} = \frac{C_{\mathbf{v}}}{E_{\mathbf{v}}} > 0, \quad c_1 = \varepsilon^{1-\delta_{\mathbf{v}}} > 0, \quad g_{\mathbf{v}} = \frac{\alpha_{\mathbf{v}}}{E_{\mathbf{v}}} > 0 \quad \text{and} \quad c_2 = g_{\mathbf{v}} \ln(\varepsilon).$$

Similarly, points (r, φ) in $In(\mathbf{w}) \setminus W^s(\mathbf{w})$ leave W at $Out(\mathbf{w})$ at:

$$\Phi_{\mathbf{w}}(r, \varphi) = (c_3 - g_{\mathbf{w}} \ln r + \varphi, c_4 r^{\delta_{\mathbf{w}}}) = (x, y), \quad (4.2)$$

where $\delta_{\mathbf{w}}$ is the *saddle index* of \mathbf{w} ,

$$\delta_{\mathbf{w}} = \frac{C_{\mathbf{w}}}{E_{\mathbf{w}}} > 0, \quad g_{\mathbf{w}} = -\frac{\alpha_{\mathbf{w}}}{E_{\mathbf{w}}} < 0, \quad c_3 = g_{\mathbf{w}} \ln \varepsilon \quad \text{and} \quad c_4 = \varepsilon^{1-\delta_{\mathbf{w}}} > 0.$$

The minus sign in the equation $\dot{\theta} = -\alpha_{\mathbf{w}}$ of (4.1) corresponds to the hypothesis (P4) and this implies that $g_{\mathbf{w}} < 0$.

4.5 Geometry near the cycle

The notation and constructions of this section may now be used to describe the geometry associated to the local dynamics around the cycle. We start with some definitions that help the geometric description near each saddle-focus, illustrated in Figure 4.

Definition 2 1. A segment β in $In(\mathbf{v})$ or $Out(\mathbf{w})$ is a smooth regular parametrised curve of the type

$$\beta : (0, 1] \rightarrow In(\mathbf{v}) \quad \text{or} \quad \beta : (0, 1] \rightarrow Out(\mathbf{w})$$

that meets $W_{loc}^s(\mathbf{v})$ or $W_{loc}^u(\mathbf{w})$ transversely at the point $\beta(0)$ only and such that, writing $\beta(s) = (x(s), y(s))$, both x and y are monotonic and bounded functions of s and $\frac{dx}{ds}$ is bounded.

2. A spiral in $Out(\mathbf{v})$ or $In(\mathbf{w})$ around a point p is a curve

$$\alpha : (0, 1] \rightarrow Out(\mathbf{v}) \quad \text{or} \quad \alpha : (0, 1] \rightarrow In(\mathbf{w})$$

satisfying $\lim_{s \rightarrow 0^+} \alpha(s) = p$ and such that, if $\alpha(s) = (\alpha_1(s), \alpha_2(s))$ are its expressions in polar coordinates (ρ, θ) around p , then α_1 and α_2 are monotonic, with $\lim_{s \rightarrow 0^+} |\alpha_2(s)| = +\infty$.

3. Consider a cylinder C parametrised by a covering $(\theta, h) \in \mathbf{R} \times [a, b]$, with $a < b \in \mathbf{R}$ where θ is periodic. A helix in the cylinder C accumulating on the circle $h = h_0$ is a curve $\gamma : (0, 1] \rightarrow C$ such that its coordinates $(\theta(s), h(s))$ satisfy

$$\lim_{s \rightarrow 0^+} h(s) = h_0 \quad , \quad \lim_{s \rightarrow 0^+} |\theta(s)| = +\infty$$

and the maps θ and h are monotonic.

We are interested in spirals for which the point p in the definition is the intersection of the two-dimensional local stable/unstable manifold of \mathbf{v} or \mathbf{w} with the cross section. The next lemma from Aguiar *et al* [4, Section 6] summarises some basic results on the geometry near the saddle-foci. In its original form the authors assume implicitly that property (P4) does not hold, we make the necessary adaptations.

Lemma 7 (Aguiar *et al* [4]) A segment β :

1. in $In(\mathbf{v})$ is mapped by $\Phi_{\mathbf{v}}$ into a spiral in $Out(\mathbf{v})$ around $W^u(\mathbf{v})$;
2. in $Out(\mathbf{w})$ is mapped by $\Phi_{\mathbf{w}}^{-1}$ into a spiral in $In(\mathbf{w})$ around $W^s(\mathbf{w})$;
3. in $In(\mathbf{v})$ is mapped by $\Phi_{\mathbf{v}}$ into a spiral in $Out(\mathbf{v})$ around $W^u(\mathbf{v})$, that is mapped by $\Psi_{\mathbf{v} \rightarrow \mathbf{w}}$ into another spiral around $W^s(\mathbf{w}) \cap In(\mathbf{v})$.

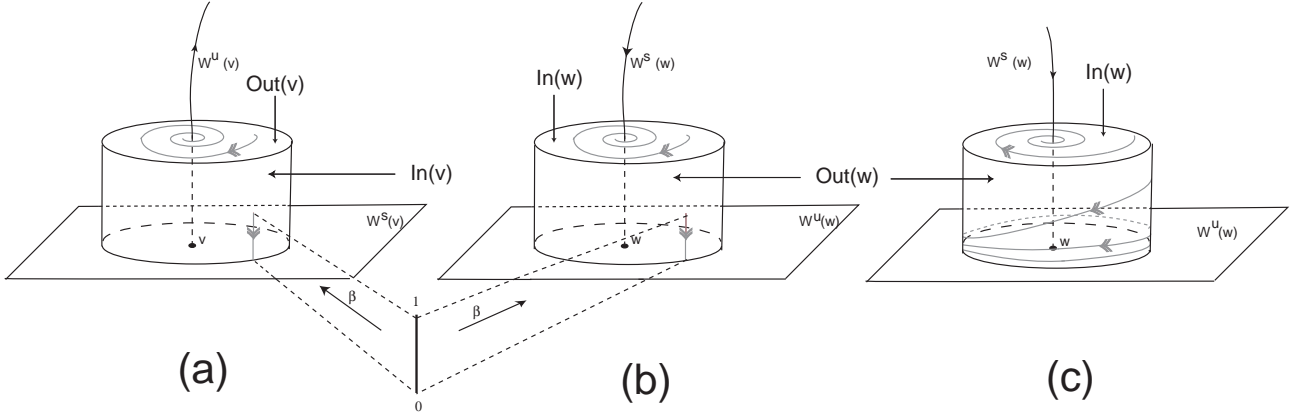


Figure 4: Smooth structures referred in Lemma 7. The double arrows on the gray curves (segment, spiral and helix) indicate correspondence of orientation and not the flow. (a) A segment β in $In(\mathbf{v})$ is mapped by $\Phi_{\mathbf{v}}$ into a spiral in $Out(\mathbf{v})$ around $W^u(\mathbf{v})$. (b) A segment β in $Out(\mathbf{w})$ is mapped by $\Phi_{\mathbf{w}}^{-1}$ into a spiral in $In(\mathbf{w})$ around $W^s(\mathbf{w})$. (c) If (P4) does not hold, a spiral in $In(\mathbf{w})$ around $W^s(\mathbf{w})$ is mapped by $\Phi_{\mathbf{w}}$ into a helix in $Out(\mathbf{w})$ accumulating on the circle $Out(\mathbf{w}) \cap W^u(\mathbf{w})$. For the behaviour when (P4) holds see Figure 6.

4. If (P4) does not hold, this last spiral is mapped by $\Phi_{\mathbf{w}}$ into a helix in $Out(\mathbf{w})$ accumulating on the circle $Out(\mathbf{w}) \cap W^u(\mathbf{w})$.

The transition map $\Psi_{\mathbf{v}, \mathbf{w}}$ has a simple geometry as depicted in Figure 5.

Lemma 8 A circle of radius $r < \varepsilon$ in $Out(\mathbf{v})$ centered at the origin is mapped by $\Psi_{\mathbf{v}, \mathbf{w}}$ into an ellipse centered at the origin of $In(\mathbf{w})$ with major axis of length $ar \geq r$ and minor axis of length $\frac{r}{a} \leq r$.

Note that the map $\Psi_{\mathbf{v}, \mathbf{w}}$ is given in rectangular coordinates. To compose this map with $\Phi_{\mathbf{w}}$, it is required to change the coordinates. We address this issue in Section 5.

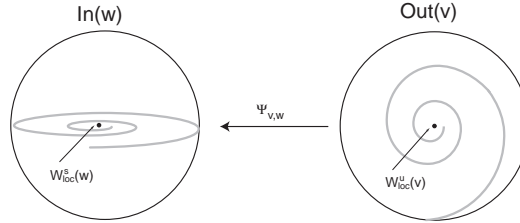


Figure 5: The transition map from V to W may be approximated by $\Psi_{\mathbf{v}, \mathbf{w}}(x, y) = (ax, y/a)$, where (x, y) are the rectangular coordinates at $Out(\mathbf{v})$ and $In(\mathbf{w})$. A circle with centre at $W^s_{loc}(\mathbf{v})$ is mapped into an ellipse and a spiral is deformed in a similar way.

5 Heteroclinic Tangencies and Horseshoes

In this section we give a more precise formulation of Theorems 1 and 2 and prove them. In order to simplify computations, we assume from now on, that $W^u(\mathbf{w}) \cap In(\mathbf{v})$ and $W^s(\mathbf{v}) \cap Out(\mathbf{w})$ are vertical segments across $In(\mathbf{v})$ and $Out(\mathbf{w})$, respectively. Let $\beta(s) = (0, s) \subset In(\mathbf{v})$, $s \in [0, \varepsilon]$, be a parametrisation of $W^u(\mathbf{w}) \cap In(\mathbf{v})$, where $(0, 0)$ are the local coordinates of the point $[\mathbf{v} \rightarrow \mathbf{w}] \cap In(\mathbf{v})$. Then

$$\Phi_{\mathbf{w}} \circ \Psi_{\mathbf{v}, \mathbf{w}} \circ \Phi_{\mathbf{v}}(\beta(s))$$

defines an oriented curve in $Out(\mathbf{w})$ with the properties of Lemma 7. Our first step is to show that this curve changes the direction of its turning around the cylinder $Out(\mathbf{w})$ at infinitely many points where it has a vertical tangent.

5.1 Preliminary analysis of maps

In this subsection we obtain the expression for $\Phi_{\mathbf{w}} \circ \Psi_{\mathbf{v}, \mathbf{w}} \circ \Phi_{\mathbf{v}}(\beta(s))$. The following result is a generalization of Ovsyannikov and Shilnikov [35], treating the dependence on a and containing simpler expressions.

Lemma 9 *Let $\beta = (0, s)$, $s \in [0, \varepsilon]$, be a segment in $In(\mathbf{v})$ parametrized by s where*

$$\{(0, 0)\} = [\mathbf{w} \rightarrow \mathbf{v}] \cap In(\mathbf{v})$$

and let $(x_{\mathbf{w}}(s), y_{\mathbf{w}}(s)) = \Phi_{\mathbf{w}} \circ \Psi_{\mathbf{v}, \mathbf{w}} \circ \Phi_{\mathbf{v}}(\beta(s))$. Then:

$$\begin{cases} x_{\mathbf{w}}(s) = -g_{\mathbf{w}}\delta_{\mathbf{v}} \ln s - \frac{g_{\mathbf{w}}}{2} \ln C(\varphi) + \Phi(\varphi) + c_3 - g_{\mathbf{w}} \ln c_1 \\ y_{\mathbf{w}}(s) = c_4 c_1^{\delta_{\mathbf{v}}\delta_{\mathbf{w}}} s^{\delta_{\mathbf{v}}\delta_{\mathbf{w}}} [C(\varphi)]^{\frac{\delta_{\mathbf{w}}}{2}} \end{cases} \quad (5.3)$$

where

$$\begin{aligned} \varphi(s) &= -g_{\mathbf{v}} \ln s + c_2, \\ C(\varphi) &= a^2 \cos^2(\varphi) + \frac{1}{a^2} \sin^2(\varphi) \quad \text{and} \\ \Phi(\varphi) &= \arg\left(a \cos(\varphi), \frac{1}{a} \sin(\varphi)\right), \end{aligned} \quad (5.4)$$

with the argument \arg taken in the interval $\left[\frac{k\pi}{2}, \frac{(k+1)\pi}{2}\right]$, $k \in \mathbf{Z}$ that contains φ .

Proof: The image of β under the local map near \mathbf{v} , $\Phi_{\mathbf{v}}$, is given by:

$$\Phi_{\mathbf{v}}(0, s) = (c_1 s^{\delta_{\mathbf{v}}}, -g_{\mathbf{v}} \ln s + c_2) = (r, \varphi) \quad (5.5)$$

that in rectangular coordinates has the form $(X(s), Y(s)) = (r(s) \cos \varphi(s), r(s) \sin \varphi(s))$, hence:

$$\Psi_{\mathbf{v}, \mathbf{w}} \circ \Phi_{\mathbf{v}}(0, s) = \left(a r(s) \cos \varphi(s), \frac{r(s)}{a} \sin \varphi(s)\right) \quad (5.6)$$

Therefore the radial component of $\Psi_{\mathbf{v}, \mathbf{w}} \circ \Phi_{\mathbf{v}}(\beta(s))$ may be written as $R = r(s) \sqrt{C(\varphi)}$ and the angular component is

$$\Phi = \arg\left(c_1 s^{\delta_{\mathbf{v}}} \left(a \cos(\varphi), \frac{1}{a} \sin(\varphi)\right)\right) = \arg\left(a \cos(\varphi), \frac{1}{a} \sin(\varphi)\right)$$

since $c_1 s^{\delta_{\mathbf{v}}} > 0$. Using the expression $\Phi_{\mathbf{w}}$ of the local map near \mathbf{w} it follows that $\Phi_{\mathbf{w}} \circ \Psi_{\mathbf{v}, \mathbf{w}} \circ \Phi_{\mathbf{v}}(\beta(s))$ has the form given in the statement of the lemma. \square

We can now give a description of the global dynamics near the whole network. Hereafter, denote by δ the product $\delta_{\mathbf{v}}\delta_{\mathbf{w}}$, and by η the map $\Phi_{\mathbf{w}} \circ \Psi_{\mathbf{v}, \mathbf{w}} \circ \Phi_{\mathbf{v}} : In(\mathbf{v}) \rightarrow Out(\mathbf{w})$.

Lemma 10 *Let β be a segment on $In(\mathbf{v})$ parametrized in rectangular coordinates by $(x_{\mathbf{v}}(s), y_{\mathbf{v}}(s))$ and let $(x_{\mathbf{w}}(s), y_{\mathbf{w}}(s))$ be the coordinates of $\eta(\beta(s)) \in Out(\mathbf{w})$. Then:*

1. *if $a = 1$, then the coordinates $x_{\mathbf{w}}(s)$ and $y_{\mathbf{w}}(s)$ are both monotonic functions of s ;*
2. *if $a \neq 1$, then the coordinate $y_{\mathbf{w}}(s)$ is not a monotonic function of s ;*
3. *for any $a \neq 0$, we have $\lim_{s \rightarrow 0^+} y_{\mathbf{w}}(s) = 0$;*
4. *let $\gamma = \frac{\alpha_{\mathbf{w}}}{\alpha_{\mathbf{v}}} \frac{C_{\mathbf{v}}}{E_{\mathbf{w}}}$, then for any $a \neq 0$, if $\gamma > 1$ then $\lim_{s \rightarrow 0^+} x_{\mathbf{w}}(s) = -\infty$ and if $0 < \gamma < 1$ then $\lim_{s \rightarrow 0^+} x_{\mathbf{w}}(s) = +\infty$*

Proof:

1. If $a = 1$, then $C(\varphi) = a^2 \cos^2(\varphi) + \frac{1}{a^2} \sin^2(\varphi) \equiv 1$. Hence, $y_{\mathbf{w}}(s) = k_1 s^\delta$, where $k_1 \in \mathbf{R}^+$ and the result follows directly. Since $a = 1$, we may write $x_{\mathbf{w}}(s) = k_2 - (g_{\mathbf{w}}\delta_{\mathbf{v}} + g_{\mathbf{v}}) \ln s = k_2 - \frac{\alpha_{\mathbf{v}}}{E_{\mathbf{v}}} (1 - \gamma) \ln s$, where $k_2 \in \mathbf{R}^+$, then $x_{\mathbf{w}}(s)$ is monotonic. If $\gamma \neq 1$ then $x_{\mathbf{w}}(s)$ is strictly monotonic.

2. If $a \neq 1$, then $y_{\mathbf{w}}(s)$ is not monotonic because, in $In(\mathbf{w})$, the euclidean distance between $\Psi_{\mathbf{v}, \mathbf{w}} \circ \Phi_{\mathbf{v}}(\beta(s))$ and $W^s(\mathbf{w})$ is not a decreasing function of the parameter s . Thus, the map $y_{\mathbf{w}}(s)$ that represents the height is not monotonic. Recall that $\Psi_{\mathbf{v}, \mathbf{w}}$ consists of an expansion in the horizontal direction and a contraction in the vertical direction.

3. Since $(C(\varphi))^{\frac{\delta_{\mathbf{w}}}{2}} = (a^2 \cos^2(\varphi) + \frac{1}{a^2} \sin^2(\varphi))^{\frac{\delta_{\mathbf{w}}}{2}}$ is bounded, then $\lim_{s \rightarrow +\infty} y_{\mathbf{w}}(s) = \lim_{s \rightarrow +\infty} k_1 s^{\delta_{\mathbf{v}}} = 0$.

4. Let $\hat{x}(s) = -g_{\mathbf{w}}\delta_{\mathbf{v}} \ln s + \Phi(\varphi(s))$. Note that $\hat{x}(s) - x_{\mathbf{w}}(s) = -\frac{g_{\mathbf{w}}}{2} \ln C(\varphi) + c_3 - g_{\mathbf{w}} \ln c_1$ is limited, hence it is sufficient to compute $\lim_{s \rightarrow 0^+} \hat{x}(s)$.

Since $\lim_{s \rightarrow 0^+} \varphi(s) = +\infty$, then as $s \rightarrow 0^+$ one gets $\frac{2}{\pi} \varphi(s) \in [k, k+1]$ with $k \in \mathbf{N}$, $k \rightarrow +\infty$ and thus $\frac{2}{\pi} \Phi(s)$ lies in the same interval. Using $-g_{\mathbf{w}}\delta_{\mathbf{v}} \ln s = \frac{g_{\mathbf{w}}\delta_{\mathbf{v}}}{g_{\mathbf{v}}} \varphi(s) = -\gamma \varphi(s)$ it follows that $\frac{2}{\pi} \hat{x}(s) \in [(1-\gamma)k - \gamma, (1-\gamma)k + 1]$. Hence, if $0 < \gamma < 1$ then $\lim_{s \rightarrow 0^+} \hat{x}(s) = +\infty$, and if $\gamma > 1$ then $\lim_{s \rightarrow 0^+} \hat{x}(s) = -\infty$. \square

The dynamics in the reversible case, when $\gamma = 1$, has been described in [29].

5.2 The reversal property

The main goal now is to prove that under hypothesis (P1)–(P4), the coordinate map $x_{\mathbf{w}}$ is not a monotonic function of s , since the curve $\eta \circ \beta$ reverses the direction of its turning around $Out(\mathbf{w})$ infinitely many times. This is the notion behind the following definition:

Definition 3 *We say that the vector field f has the dense reversals property if for the vertical segment $\beta(s) = (0, s) \in In(\mathbf{v})$, $s \in [0, \varepsilon]$, the projection into $W_{loc}^u(\mathbf{w})$ of the points where $\eta \circ \beta$ has a vertical tangent is dense in $W_{loc}^u(\mathbf{w}) \cap Out(\mathbf{w})$.*

The dense reversals property is the key step in the proof of Theorem 1. In order to prove it we need some additional assumptions on the parameters $P = (\alpha_{\mathbf{v}}, C_{\mathbf{v}}, E_{\mathbf{v}}, \alpha_{\mathbf{w}}, C_{\mathbf{w}}, E_{\mathbf{w}})$, that determine the linear part of the vector field f at the equilibria. Note that Case 1 of Lemma 10 rules out reversals when $a = 1$. For any $a > 1$, let \mathcal{B} be the subset of parameters given by:

$$\mathcal{B} = \left\{ P : \left(a^2 - \frac{1}{a^2} \right) \frac{2\alpha_{\mathbf{v}}}{C_{\mathbf{v}} - \sqrt{\alpha_{\mathbf{v}}^2 + 4C_{\mathbf{v}}^2}} \leq \frac{E_{\mathbf{w}}}{\alpha_{\mathbf{w}}} - \frac{a^2 C_{\mathbf{v}}}{\alpha_{\mathbf{v}}} \leq \left(a^2 - \frac{1}{a^2} \right) \frac{2\alpha_{\mathbf{v}}}{C_{\mathbf{v}} + \sqrt{\alpha_{\mathbf{v}}^2 + 4C_{\mathbf{v}}^2}} \right\} \quad (5.7)$$

and having non empty interior $int(\mathcal{B})$. Let \mathcal{D} be the dense subset of \mathcal{B} given by:

$$\mathcal{D} = \left\{ P \in int(\mathcal{B}) : \gamma = \frac{\alpha_{\mathbf{w}}}{\alpha_{\mathbf{v}}} \frac{C_{\mathbf{v}}}{E_{\mathbf{w}}} \notin \mathbf{Q} \right\}. \quad (5.8)$$

The condition (5.7) in the definition of \mathcal{B} is satisfied by an open set of parameters $\alpha_{\mathbf{v}}, C_{\mathbf{v}}, \alpha_{\mathbf{w}}, E_{\mathbf{w}}$ and does not involve the quantities $E_{\mathbf{v}}$ and $C_{\mathbf{w}}$. The condition (5.8) defining \mathcal{D} also does not involve $E_{\mathbf{v}}$ and $C_{\mathbf{w}}$ and hence \mathcal{D} has full Lebesgue measure in the open set $int(\mathcal{B})$. The next result shows that the dense reversals property is generic in the class of vector fields that satisfy (P1)–(P4) with parameters in \mathcal{B} . This will be used to complete the proof Theorem 1.

Theorem 11 *Let f be a vector field on \mathbf{S}^3 satisfying (P1)–(P4). If the parameters for the linear part of f near \mathbf{v} and \mathbf{w} lie in \mathcal{D} with $a > 1$ then f has the dense reversals property.*

Proof: We need to compute the coordinate $x_{\mathbf{w}}(s)$ at the points where $\eta(\beta(s))$ has a vertical tangent, where $\beta(s) = (0, s) \subset In(\mathbf{v})$, $s \in [0, \varepsilon]$ is a parametrisation of a vertical segment. Differentiating the

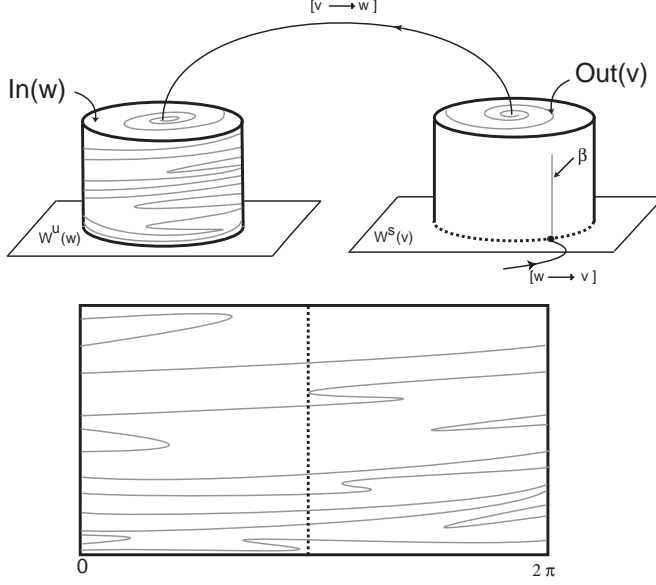


Figure 6: Top: the vertical segment β on $In(v)$ is mapped by $\Psi_{v,w} \circ \Phi_v$ into a distorted spiral in $In(w)$ and by η into a curve in $Out(w)$ that accumulates on $W^u(w)$. Bottom: on the cross section $Out(w)$, the curve $\eta \circ \beta$ reverses the orientation of its angular coordinate infinitely many times as it accumulates on $W^u(w)$ and crosses $W^s(v)$ (dotted line) infinitely many times. The angular coordinates of the points of reversal are dense in the circle, small changes in $W^s(v) \cap Out(w)$ create tangencies that coexist with transverse crossings of the invariant manifolds.

expression (5.3) of Lemma 9, we get:

$$\frac{dx_w}{ds} = -\frac{1}{s} \left[g_w \delta_v + \frac{1}{C(\varphi)} \left(2g_w g_v \left(a^2 - \frac{1}{a^2} \right) \sin \varphi \cos \varphi + g_v \right) \right] \quad (5.9)$$

and hence $dx_w/ds = 0$ has solutions if and only if $A(\varphi) = \alpha_v E_w / \alpha_w$ where

$$A(\varphi) = C_v a^2 \cos^2 \varphi + \frac{C_v}{a^2} \sin^2 \varphi + 2\alpha_v \left(a^2 - \frac{1}{a^2} \right) \sin \varphi \cos \varphi. \quad (5.10)$$

Therefore $dx_w/ds = 0$ has solutions (see Figure 7) if and only if

$$\min A(\varphi) \leq \frac{\alpha_v E_w}{\alpha_w} \leq \max A(\varphi). \quad (5.11)$$

In order to determine the maxima and the minima of $A(\varphi)$, we compute:

$$\frac{dA}{d\varphi} = 2 \left(a^2 - \frac{1}{a^2} \right) [\alpha_v \cos^2 \varphi - C_v \cos \varphi \sin \varphi - \alpha_v \sin^2 \varphi] = 2 \left(a^2 - \frac{1}{a^2} \right) \mathcal{Q}(\cos \varphi, \sin \varphi),$$

where $\mathcal{Q}(x, y) = \alpha_v x^2 - C_v xy - \alpha_v y^2$. The quadratic form $\mathcal{Q}(x, y)$ equals zero on the lines that join the origin to the points

$$(x_\star^\pm, y_\star) = (C_v \pm \sqrt{C_v^2 + 4\alpha_v^2}, 2\alpha_v).$$

Hence

$$\frac{dA}{d\varphi} = 0 \quad \Leftrightarrow \quad (\cos \varphi_\star^\pm, \sin \varphi_\star^\pm) = \frac{1}{N} (x_\star^\pm, y_\star) \quad \text{with} \quad N = \|(x_\star^\pm, y_\star)\|.$$

In order to impose condition (5.11), we write $A(\varphi) = \mathcal{R}(\cos \varphi, \sin \varphi)$ where

$$\mathcal{R}(x, y) = C_v a^2 x^2 + 2\alpha_v \left(a^2 - \frac{1}{a^2} \right) xy + \frac{C_v}{a^2} y^2.$$

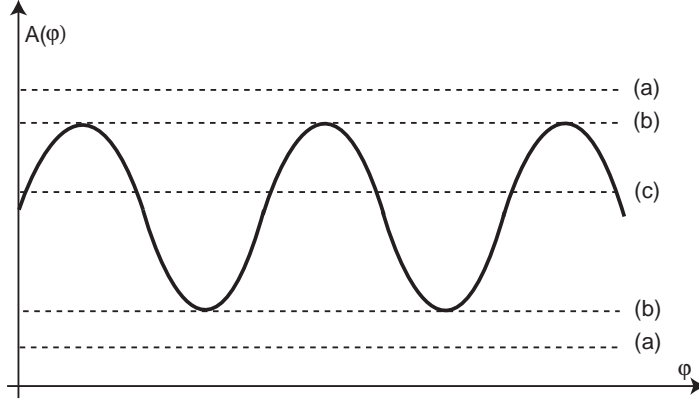


Figure 7: Positions of the graph of $A(\varphi)$ of (5.10) (solid curve) with respect to different values of $\alpha_v E_{\mathbf{w}}/\alpha_{\mathbf{w}}$ (dashed lines). Parameters outside the set \mathcal{B} of (5.7) correspond to cases (a), where the graph of $A(\varphi)$ never crosses the dashed line, and hence $x_{\mathbf{w}}(s)$ is a monotonic function of s . Cases (b) and (c) correspond to parameters in \mathcal{B} . Points where $x_{\mathbf{w}}(s)$ has a vertical tangent are created in case (b) as the graph of $A(\varphi)$ is tangent to the dashed line, for parameters in the boundary of \mathcal{B} . The graph of $A(\varphi)$ crosses the dashed line transversely in case (c) for parameters in the interior of \mathcal{B} , giving rise to two π -periodic sequences of points of vertical tangency.

Since $\mathcal{R}(x, y) > 0$ if $x > 0$ and $y > 0$, then (x_{\star}^+, y_{\star}) corresponds to maxima of $A(\varphi)$ and (x_{\star}^-, y_{\star}) to minima.

Let $S = \sqrt{C_{\mathbf{v}} + 4\alpha_{\mathbf{v}}^2}$, then

$$N^2 = 2C_{\mathbf{v}}^2 + 8\alpha_{\mathbf{v}}^2 \pm 2C_{\mathbf{v}}S = 2S(S \pm C_{\mathbf{v}})$$

and

$$\mathcal{R}(x_{\star}^{\pm}, y_{\star}) = C_{\mathbf{v}}a^2N^2 \pm 2\alpha_{\mathbf{v}}^2 \left(a^2 - \frac{1}{a^2} \right) S$$

and hence

$$A(\varphi_{\star}^{\pm}) = \frac{1}{N^2} \mathcal{R}(x_{\star}^{\pm}, y_{\star}) = a^2C_{\mathbf{v}} \pm 2\alpha_{\mathbf{v}}^2 \left(a^2 - \frac{1}{a^2} \right) \frac{S}{2S(S \pm C_{\mathbf{v}})} = a^2C_{\mathbf{v}} + 2\alpha_{\mathbf{v}}^2 \left(a^2 - \frac{1}{a^2} \right) \frac{1}{C_{\mathbf{v}} \pm S},$$

showing that conditions (5.7) and (5.11) are equivalent. These conditions imply that $A(\varphi) = \alpha_{\mathbf{v}}E_{\mathbf{w}}/\alpha_{\mathbf{w}}$ at infinitely many values $\varphi = \varphi_0 + n\pi$, where $\varphi_0 \in [0, \pi]$ and $n \in \mathbf{Z}$. Since $\varphi = -g_{\mathbf{v}} \ln s + c_2$, then $dx_{\mathbf{w}}/ds = 0$ has solutions $s_n = s_0 e^{-\frac{n\pi}{g_{\mathbf{v}}}}$, $n = 0, 1, 2, \dots$ where $s_0 = e^{-\frac{\varphi_0}{g_{\mathbf{v}}} e^{\frac{c_2}{g_{\mathbf{v}}}}}$. In Lemma 12 below, we show that $x_{\mathbf{w}}(s_n) = x_{\mathbf{w}}(s_0) + n\pi(1 - \gamma)$. Hence, if the genericity condition $\gamma \notin \mathbf{Q}$ in (5.8) holds, then the points $x_{\mathbf{w}}(s_n)$ are dense in the circle defined by $W_{loc}^u(\mathbf{w}) \cap Out(\mathbf{w})$.

By the implicit function theorem, the arguments that we have used for vertical tangencies are still valid if $\beta(s)$ is any line with slope close to the vertical. \square

Lemma 12 *For any $s_0 \in \mathbf{R}$ and $n = 0, 1, 2, \dots$, we have*

$$x_{\mathbf{w}} \left(s_0 e^{-\frac{n\pi}{g_{\mathbf{v}}}} \right) = x_{\mathbf{w}}(s_0) + n\pi(1 - \gamma) \quad \text{for} \quad \gamma = \frac{\alpha_{\mathbf{w}} C_{\mathbf{v}}}{\alpha_{\mathbf{v}} E_{\mathbf{w}}}. \quad (5.12)$$

Proof: Using the expressions (5.4) we get that $\varphi(s) = \varphi(s_0) + n\pi$ and $C(\varphi + \pi) = C(\varphi)$. Also, if $\varphi(s) \in \left[\frac{k\pi}{2}, \frac{(k+1)\pi}{2} \right]$, then $\Phi(\varphi)$ lies in the same interval and $\Phi(\varphi + \pi) = \Phi(\varphi) + \pi$. The result follows, using the expression (5.3) for $x_{\mathbf{w}}(s)$ in Lemma 9. \square

The next theorem is a precise formulation of Theorem 1.

Theorem 13 *Let \mathcal{A}_P be the set of vector fields on \mathbf{S}^3 satisfying (P1)–(P4), for a given parameter value $P \in \mathcal{B}$. Then there is an open subset \mathcal{C} of \mathcal{A}_P such that the set of vector fields in \mathcal{C} whose flow has tangencies between the two dimensional invariant manifolds $W^u(\mathbf{w})$ and $W^s(\mathbf{v})$ is dense in \mathcal{A}_P in the C^k topology, for every $k \geq 2 \in \mathbf{N}$.*

Proof: As in the proof of Theorem 11, suppose that $W^u(\mathbf{w}) \cap \text{In}(\mathbf{v})$ and $W^s(\mathbf{v}) \cap \text{Out}(\mathbf{w})$ are vertical segments across $\text{In}(\mathbf{v})$ and $\text{Out}(\mathbf{w})$, respectively. Let $\beta(s) = (0, s) \subset \text{In}(\mathbf{v})$, $s \in (0, \varepsilon]$, be a parametrisation of $W^u(\mathbf{w}) \cap \text{In}(\mathbf{v})$, where $(0, 0)$ is the point $[\mathbf{v} \rightarrow \mathbf{w}] \cap \text{In}(\mathbf{v})$ and let $\gamma(s) = (x_0, s)$, $s \in (0, \varepsilon]$ be a parametrisation of $W^s(\mathbf{v}) \cap \text{Out}(\mathbf{w})$, where $(0, 0)$ is the point $[\mathbf{v} \rightarrow \mathbf{w}] \cap \text{Out}(\mathbf{w})$.

If x_0 is the projection of a point where $\eta \circ \beta$ has a vertical tangent, then $W^s(\mathbf{v})$ is tangent to $W^u(\mathbf{w})$ at the corresponding point. Otherwise, by Theorem 11, an arbitrarily small modification of the vector field f in a neighbourhood of $(x_0, 0)$ will move x_0 , creating the tangency.

As remarked before, the proof of Theorem 13 still holds if $W^u(\mathbf{w}) \cap \text{In}(\mathbf{v})$ is a line with slope close to the vertical, and hence we still have the dense reversals property in this case, as we proceed to explain. Suppose $W^s(\mathbf{v}) \cap \text{Out}(\mathbf{w})$ is a curve close to a vertical segment and that it is parametrised by $\xi(s) = (x(s), y(s))$, with $\xi(0) = (x_0, 0)$. Then, changing f near $(x_0, 0)$ if necessary, we may assume that $\xi(s)$ meets $\eta \circ \beta$ at a point where the last curve has a vertical tangent. Since ξ is close to a vertical line, then its slope near the intersection is close to the vertical, so a small change of the vector field near this point will create a tangency. \square

5.3 Topological and Hyperbolic Horseshoes

In this section we give the geometrical construction for the proof of Theorem 2. This is the standard construction for establishing symbolic dynamics, except for the obstacle of infinitely many reversions, that we will overcome by showing that the non-transverse intersections can be avoided, since generically the line $\eta \circ \beta(s)$ intersects transversally $W_{loc}^s(\mathbf{v}) \cap \text{Out}(\mathbf{w})$ infinitely many times. This phenomenon coexists with the denseness of the tangencies in \mathcal{A}_P .

First we need to recall some terminology about horizontal and vertical strips used in Guckenheimer and Holmes [19] adapted to our purposes. Given a rectangle $[w_1, w_2] \times [z_1, z_2]$ in either $\text{In}(\mathbf{v})$ or $\text{Out}(\mathbf{w})$, a *horizontal strip* across the rectangle is the set

$$\{(x, y) : x \in [w_1, w_2], y \in [u_1(x), u_2(x)]\},$$

where $u_1, u_2 : [w_1, w_2] \rightarrow [z_1, z_2]$ are Lipschitz functions such that $u_1(x) < u_2(x)$. The *horizontal boundaries* of the strip are the graphs of the u_i and the *vertical boundaries* are the lines $\{w_i\} \times [u_1(w_i), u_2(w_i)]$. A *vertical strip* across the rectangle has a similar definition with the roles of x and y reversed.

Recall that $P = (\alpha_v, C_v, E_v, \alpha_w, C_w, E_w)$ is the set of parameters that determine the linear part of f at the hyperbolic saddle-foci and that $\beta(s) = (0, s) \in \text{In}(\mathbf{v})$, $s \in [0, \varepsilon]$. The next result holds for almost all vector fields on \mathbf{S}^3 satisfying (P1)–(P4). One exception is the case $\gamma = 1$, that occurs in reversible vector fields, as remarked before. The other exception occurs when $\gamma \in \mathbf{Q}$ and $P \in \mathcal{B}$ and when moreover there are points in $\text{Out}(\mathbf{w})$ with first coordinate equal to zero, where $\eta \circ \beta$ has a vertical tangent — we say in this case that the vector field has a *periodic tangency*.

Proposition 14 *If $\gamma = \frac{\alpha_w C_v}{\alpha_v E_w} \neq 1$, then for all vector fields on \mathbf{S}^3 satisfying (P1)–(P4) and not having a periodic tangency, the following holds: for any sufficiently small $\tau > 0$, there is a sequence of disjoint horizontal strips across the rectangle $[0, \tau] \times [0, \tau] \subset \text{In}(\mathbf{v})$, accumulating on $W^s(\mathbf{v})$, whose image by the first return map $\Psi_{\mathbf{w}, \mathbf{v}} \circ \eta$ is a vertical strip across $[0, \tau] \times [0, \tau]$.*

Proof: Take $(0, 0)$ as the local coordinates of the points $[\mathbf{v} \rightarrow \mathbf{w}] \cap \text{In}(\mathbf{v})$ and $[\mathbf{v} \rightarrow \mathbf{w}] \cap \text{Out}(\mathbf{w})$, as before. Start with the rectangle $[0, \tau_0] \times [0, \tau_0] \subset \text{In}(\mathbf{v})$ with $0 < \tau_0 < \min\{\pi, \varepsilon\}$. For each $t \in [0, \tau_0]$, define the family of vertical segments $\beta_t(s) = (t, s) \in \text{In}(\mathbf{v})$, and let $\beta(s) = \beta_0(s)$ with $x_w(s)$ the first coordinate of $\eta(\beta(s))$, as before. Then $\eta(\beta_t(s))$, for different t , are disjoint curves in $\text{Out}(\mathbf{w})$. We will assume from now on that $\gamma > 1$, the proof in the case $0 < \gamma < 1$ is obtained by replacing increasing functions by decreasing functions, and $-\infty$ by $+\infty$ in what follows.

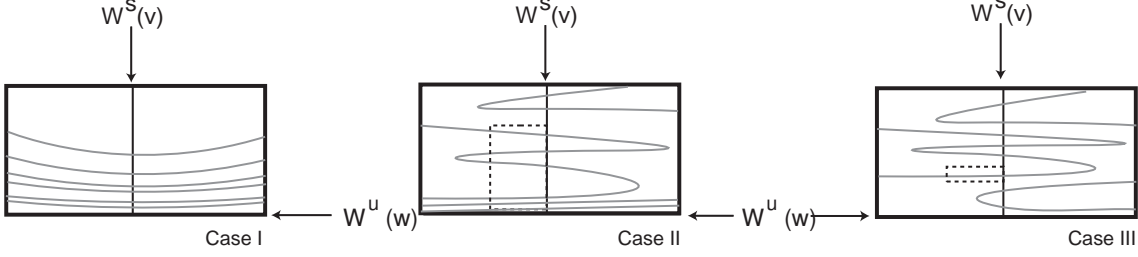


Figure 8: The curve $\eta(\beta(s)) \subset Out(\mathbf{w})$ in the three first cases of the proof of Proposition 14. **Case I:** If $P \notin \mathcal{B}$, then $x_{\mathbf{w}}(s)$ is monotonic. **Case II:** If $P \in int(\mathcal{B}) \setminus \mathcal{D}$ with $\gamma \in \mathbf{Q}$, then reversion points are periodic. **Case III:** If $P \in \mathcal{D}$, then reversion points are dense. In cases **II** and **III** we restrict the strip to the dotted rectangle to avoid reversion points.

The proof consists in finding τ with $0 < \tau \leq \tau_0$ and a decreasing sequence $s_n > 0$, with $\lim_{n \rightarrow \infty} s_n = 0$, such that in each interval (s_{2n+1}, s_{2n}) the function $x_{\mathbf{w}}(s)$ is monotonically increasing and crosses $[-\tau, 0] \pmod{2\pi}$. Hence on this interval the curve $\eta(\beta(s))$ is transverse to each vertical line in $Out(\mathbf{w})$ and for each n there are $a_n < b_n \in (s_{2n+1}, s_{2n})$ such that $x_{\mathbf{w}}(a_n) = -\tau \pmod{2\pi}$ and $x_{\mathbf{w}}(b_n) = 0 \pmod{2\pi}$.

The curves $\eta(\beta_t(s))$ have the same properties, i.e., by taking a smaller $\tau > 0$ if necessary, since the curves depends smoothly on t , the following holds: for each $t \in [0, \tau]$ there are two sequences $0 < a_n(t) < b_n(t) < a_{n-1}(t)$, with $\lim_{n \rightarrow \infty} a_n(t) = 0$, such that in each interval $[a_n(t), b_n(t)]$ the first coordinate of $\eta(\beta_t(s))$ is a monotonically increasing function of s , taking the values $-\tau \pmod{2\pi}$ at $s = a_n(t)$ and $0 \pmod{2\pi}$ at $b_n(t)$. This means that the strip across $[0, \tau] \times [0, \tau] \subset In(\mathbf{v})$ with horizontal boundaries $a_n(t)$ and $b_n(t)$ is mapped by η into a horizontal strip across $[-\tau, 0] \times [0, \tau] \subset Out(\mathbf{w})$, that in turn is mapped by $\Psi_{\mathbf{w}, \mathbf{v}}$ into a vertical strip across $[0, \tau] \times [0, \tau] \subset In(\mathbf{v})$, as required.

In order to obtain the sequence of monotonicity intervals we distinguish four cases (see Figure 8):

Case I: If $P \notin \mathcal{B}$, then the curve $\eta(\beta(s))$ does not reverse the direction of its turning around $Out(\mathbf{w})$ and $x_{\mathbf{w}}$ is a monotonically increasing function of s , since $\gamma > 1$. Using Lemma 10 it follows that $x_{\mathbf{w}}(s)$ goes across $[-\tau, 0] \pmod{2\pi}$ infinitely many times, as required.

Case II: If $P \in int(\mathcal{B}) \setminus \mathcal{D}$, then the projection into $W_{loc}^u(\mathbf{w}) \cap Out(\mathbf{w})$ of the points where the curve $\eta(\beta(s)) \in Out(\mathbf{w})$ reverses orientation is finite. Since we are assuming that the vector field does not have a periodic tangency, the curve $\eta(\beta(s))$ is never tangent to the segment $(0, s) \subset Out(\mathbf{w})$. Then there is a $\tau > 0$ such that $dx_{\mathbf{w}}/ds$ is never zero when $x_{\mathbf{w}}(s) \in [-\tau, 0] \pmod{2\pi}$ and therefore $x_{\mathbf{w}}(s)$ is a monotonic function of s when $x_{\mathbf{w}}(s)$ lies in that interval. Since $\lim_{s \rightarrow 0^+} x_{\mathbf{w}}(s) = -\infty$, it follows that $x_{\mathbf{w}}(s)$ crosses $[-\tau, 0] \pmod{2\pi}$ infinitely many times, as a monotonically increasing function of s .

Note that when the vector field has a periodic tangency we may still obtain horizontal strips in $In(\mathbf{v})$ that are mapped into vertical strips across themselves by the first return map, but there is no guarantee that their image will cross the other strips, and even less that they will cross $W_{loc}^u(\mathbf{w})$.

Case III: If $P \in \mathcal{D}$, let $\varphi_0 < \varphi_1 \in (-\pi/2, \pi/2)$ be the two solutions of $A(\varphi) - \alpha_{\mathbf{v}} E_{\mathbf{w}} / \alpha_{\mathbf{w}} = 0$ where $A(\varphi)$ is the expression (5.10) in the proof of Theorem 11 and let $d = \varphi_1 - \varphi_0 \in (0, \pi/2)$. Then all the positive solutions φ_n of $A(\varphi) - \alpha_{\mathbf{v}} E_{\mathbf{w}} / \alpha_{\mathbf{w}} = 0$ are of the form $\varphi_{2n} = \varphi_0 + n\pi$, $\varphi_{2n+1} = \varphi_1 + n\pi$. The values of $s \in (0, 1)$ where $dx_{\mathbf{w}}/ds = 0$ form the decreasing sequence $s_n = e^{-\frac{\varphi_n}{9\mathbf{v}}} e^{\frac{C_2}{9\mathbf{v}}}$ that satisfies $s_n = s_{n-2} e^{-\frac{\pi}{9\mathbf{v}}}$ for $n = 2, 3, \dots$, with $\lim_{n \rightarrow \infty} s_n = 0$. Since these are the only solutions of $dx_{\mathbf{w}}/ds = 0$, then $x_{\mathbf{w}}(s)$ is monotonic in each interval (s_{n+1}, s_n) .

From (5.9) it follows that $dx_{\mathbf{w}}/ds > 0$ if and only if $A(\varphi(s)) > C_{\mathbf{v}}/\gamma$. At $\varphi = 0$ we have $A(0) = C_{\mathbf{v}} a^2$ and this is larger than $C_{\mathbf{v}}/\gamma$ because $a > 1$ and $\gamma > 1$. Hence $dx_{\mathbf{w}}/ds > 0$ if $s \in (s_1, s_0)$. Since $A(\varphi)$ has period π , then $dx_{\mathbf{w}}/ds > 0$ for $s \in (s_{2n+1}, s_{2n})$.

From Lemma 12 it follows that $x_{\mathbf{w}}(s_{2n+1}) - x_{\mathbf{w}}(s_{2n}) = d$. As noted at the end of the proof of Theorem 11, the values of $x_{\mathbf{w}}(s_{2n+1}) \pmod{2\pi}$ correspond to an irrational rotation around the circle, so these values are dense and uniformly distributed in $[0, 2\pi)$. Therefore, given $\tau < d/2$ with $0 < \tau < \tau_0$, there exist $n_j \rightarrow \infty$ such that $x_{\mathbf{w}}(s_{2n_j+1}) \in (-\tau, 0) \pmod{2\pi}$ and hence $x_{\mathbf{w}}(s_{2n_j}) \in (0, \pi/2) \pmod{2\pi}$. Hence, for s in the intervals (s_{2n_j+1}, s_{2n_j}) the curve $x_{\mathbf{w}}(s)$ goes across $[-\tau, 0]$, as required.

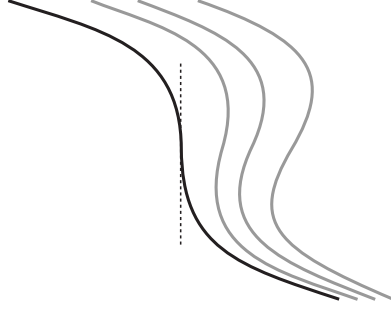


Figure 9: When the parameter P lies in $\partial\mathcal{B}$ (**Case IV**: of the proof of Proposition 14) the black curve $\eta(\beta(s))$ has a vertical tangent, but $x_{\mathbf{w}}(s)$ is still monotonic. However, grey nearby curves $\eta(\beta_t(s))$, for small $t > 0$, may reverse the direction of their turning around $Out(\mathbf{w})$.

Case IV: If $P \in \partial\mathcal{B}$, then the points where $\frac{dx_{\mathbf{w}}}{ds} = 0$ are inflection points of $x_{\mathbf{w}}(s)$. Then the curve $\eta(\beta(s))$ does not reverse the direction of its turning around $Out(\mathbf{w})$ and hence $x_{\mathbf{w}}$ is a monotonic function of s , increasing with s if $\gamma > 1$. However, nearby curves $\eta(\beta_t(s))$ for $t > 0$ may reverse their turning at pairs of points near these inflections (see Figure 9). We can choose $\tau < \tau_0$ and adapt the arguments of Cases II and III, as appropriate, to obtain inflection points of $x_{\mathbf{w}}(s)$ sufficiently far from the interval $[-\tau, 0]$, to ensure that the first coordinates of the pairs of turning points (mod 2π) do not fall in that interval. \square

Proof of Theorem 2: From Proposition 14 it follows that there is a subset of $In(\mathbf{v})$ where the first return map is semi-conjugated to a shift in an infinite set of symbols. Trajectories of points in this set return to $In(\mathbf{v})$ infinitely many times, as in assertion 1.

For assertion 2. we use the fact that each horizontal strip of Proposition 14 is mapped by the first return map $\Psi_{\mathbf{w}, \mathbf{v}} \circ \eta$ into a vertical strip across $[0, \tau] \times [0, \tau]$, and hence its image crosses $W_{loc}^s(\mathbf{v})$. Reversing the argument, we get a line of points that come from $W_{loc}^u(\mathbf{w})$, intersecting the two lines we get the 2-pulse connections. The n -pulse connections may be found iterating this argument or, alternatively, adapting the arguments of [27].

For assertion 3. we need to show that the first return map is hyperbolic, with a contracting direction. This is done in Lemma 15 below.

Using the restrictions of Proposition 14 and of Lemma 15, the set \mathcal{E} consists of those vector fields on \mathbf{S}^3 satisfying (P1)–(P4), not having a periodic tangency, for which $W_{loc}^s(\mathbf{v}) \cap Out(\mathbf{w})$ is close to a vertical line, with the restrictions $\gamma = \frac{\alpha_{\mathbf{w}} C_{\mathbf{v}}}{\alpha_{\mathbf{v}} E_{\mathbf{w}}} \neq 1$, and $\delta = \delta_{\mathbf{v}} \delta_{\mathbf{w}} = \frac{C_{\mathbf{v}} C_{\mathbf{w}}}{E_{\mathbf{v}} E_{\mathbf{w}}} > 1$. Clearly, this is an open set and $\mathcal{E} \cap \mathcal{C} \neq \emptyset$ where \mathcal{C} is the open set of Theorem 1. \square

Lemma 15 *Let $g = \Psi_{\mathbf{w}, \mathbf{v}} \circ \eta : In(\mathbf{v}) \rightarrow In(\mathbf{v})$, be the first return map of a vector field on \mathbf{S}^3 satisfying (P1)–(P4) and suppose that $\delta = \frac{C_{\mathbf{v}} C_{\mathbf{w}}}{E_{\mathbf{v}} E_{\mathbf{w}}} > 1$. Then, if one of the conditions below hold:*

1. $P \notin \mathcal{B}$;
2. $P \in \mathcal{B}$ and (x, y) lies in one of the horizontal strips of Proposition 14;

g is hyperbolic at $(x, y) \in In(\mathbf{v})$ with $y > 0$ sufficiently small.

Proof: From the expressions in Section 4 we get

$$\det Dg(x, y) = c_1^{\delta_{\mathbf{w}}} \delta y^{\delta-1} C(\varphi)^{-1+\delta_{\mathbf{w}}/2} \left(1 + (c_4 - 1) g_{\mathbf{w}}(a^2 - \frac{1}{a^2}) \sin \varphi \cos \varphi \right)$$

and since $1/a^2 \leq C(\varphi) \leq a^2$, then $C(\varphi)$ is limited and we have $\lim_{y \rightarrow 0^+} \det Dg(x, y) = 0$ if $\delta > 1$. So, for small $y > 0$, the derivative $Dg(x, y)$ has at least one contracting eigenvalue.

The trace of $Dg(x, y)$ is

$$\text{Tr } Dg(x, y) = -c_1^{\delta_{\mathbf{w}}} \delta_{\mathbf{w}} y^{\delta} C(\varphi)^{-1+\delta_{\mathbf{w}}/2} \left(a^2 - \frac{1}{a^2} \right) \sin \varphi \cos \varphi + \frac{1}{y} \frac{\alpha_{\mathbf{w}}}{E_{\mathbf{w}} E_{\mathbf{v}} C(\varphi)} \left(A(\varphi) - \frac{\alpha_{\mathbf{v}} E_{\mathbf{w}}}{\alpha_{\mathbf{w}}} \right)$$

and we want to compute $\lim_{y \rightarrow 0} \text{Tr } Dg(x, y)$. Since $\delta > 1$, the first summand tends to 0 as y tends to 0, and the second summand dominates the limit. For the second summand, we need to look at the parameters P in the equation. If $P \notin \mathcal{B}$ then $A(\varphi) - \frac{\alpha_{\mathbf{v}} E_{\mathbf{w}}}{\alpha_{\mathbf{w}}} \neq 0$ has constant sign, and therefore $\lim_{y \rightarrow 0} \text{Tr } Dg(x, y) = \pm \infty$. In this case it follows that, for small $y > 0$ and any x , the derivative $Dg(x, y)$ has one contracting and one expanding eigenvalue.

For $P \in \mathcal{B}$, the expression $A(\varphi) - \frac{\alpha_{\mathbf{v}} E_{\mathbf{w}}}{\alpha_{\mathbf{w}}} \neq 0$ does not have constant sign in general, but it does have the same sign inside each one of the horizontal strips of Proposition 14. Without loss of generality, suppose it is positive. If (x_n, y_n) is any sequence contained in the union of those strips and satisfying $\lim_{n \rightarrow \infty} y_n = 0$, then we have $\lim_{n \rightarrow \infty} \text{Tr } Dg(x_n, y_n) = \infty$, and hence for (x, y) inside a strip with small $y > 0$, the derivative $Dg(x, y)$ has one contracting and one expanding eigenvalue. \square

When $P \in \mathcal{B}$, the conclusion of Lemma 15 only holds inside the horizontal strips, because they exclude the tangencies of $W_{loc}^s(\mathbf{v})$ and $W_{loc}^u(\mathbf{w})$. Near the points where $\beta(s)$ has a vertical tangent, one may find sequences (x_n, y_n) with $\lim_{n \rightarrow \infty} y_n = 0$ for which $\lim_{n \rightarrow \infty} \text{Tr } Dg(x_n, y_n)$ takes any value between $+\infty$ and $-\infty$. In particular, there are sequences for which $\lim_{n \rightarrow \infty} \text{Tr } Dg(x_n, y_n) = 0$. At points in such a sequence $Dg(x_n, y_n)$ has two contracting eigenvalues, and this may be additional evidence for the existence of sinks, predicted by Newhouse's results. Any neighbourhood of the tangency will contain points where the first return map is not hyperbolic, at which one of the eigenvalues crosses the unit circle.

6 Example

In this section we construct a vector field in \mathbf{S}^3 that satisfies properties (P1) and (P4) and has a connection of one-dimensional invariant manifolds as in (P2). As far as we know, no explicit examples of differential equations satisfying (P1)–(P4) have been described in the literature, although these conditions follow from the set of properties described by Turaev and Shilnikov [45]. We present some evidence that the two-dimensional invariant manifolds intersect transversely, as in (P3), and we use the vector field to obtain numerical simulations that illustrate our results. Our construction is based on properties of differential equations with symmetry, we refer the reader to Golubitsky *et al* [14] for more information on the subject.

6.1 Construction of the example

We use a technique presented in Aguiar *et al* [3] that consists essentially in three steps. Start with a symmetric vector field on \mathbf{R}^3 with an attracting flow-invariant two-sphere containing a heteroclinic network. The heteroclinic network involves equilibria and one-dimensional heteroclinic connections that correspond to the intersection of fixed-point subspaces with the invariant sphere. If one of the symmetries of the vector field in \mathbf{R}^3 is a reflection, then it can be lifted by a rotation to an $\mathbf{SO}(2)$ -equivariant vector field in \mathbf{R}^4 . The sphere \mathbf{S}^3 is flow-invariant and attracting for the lifted vector field, and a two-sphere of heteroclinic connections arises from one-dimensional heteroclinic connections lying outside the plane fixed by the reflection. Perturbing the vector field in a way that destroys the $\mathbf{SO}(2)$ -equivariance and maintains the invariance of the three-sphere breaks the two-dimensional heteroclinic connection into a transverse intersection of invariant manifolds.

The first step in the construction of [3, 40] is to obtain the differential equation in \mathbf{R}^3

$$\begin{cases} \dot{x} = x(1 - r^2) - \alpha_1 xz + \alpha_2 xz^2 \\ \dot{y} = y(1 - r^2) + \alpha_1 yz + \alpha_2 yz^2 \\ \dot{z} = z(1 - r^2) + \alpha_1(z^2 - x^2) - \alpha_2 z(x^2 + y^2) \end{cases} \quad r^2 = x^2 + y^2 + z^2 \quad (6.13)$$

that has symmetries

$$\kappa_1(x, y, z) = (-x, y, z) \quad \text{and} \quad \kappa_2(x, y, z) = (x, -y, z).$$

The unit sphere \mathbf{S}^2 is flow-invariant and globally attracting, and $(0, 0, \pm 1)$ are equilibria. From the symmetry it follows that the planes $x = 0$ and $y = 0$ are flow-invariant, and hence they meet \mathbf{S}^2 in two flow-invariant circles connecting the equilibria $(0, 0, \pm 1)$. If $\alpha_2 < 0 < \alpha_1$ with $\alpha_1 + \alpha_2 > 0$, then these two equilibria are saddles, and there are heteroclinic trajectories going from each equilibrium to the other one, see [3, 40].

Now we adapt the second step in [3, 40] to obtain property (P4). Add to (6.13) a fourth coordinate θ and the equation $\dot{\theta} = z$. Taking (x, θ) as polar coordinates and rewriting the result in rectangular coordinates $X = (x_1, x_2, x_3, x_4) = (x \cos \theta, x \sin \theta, y, z)$, yields a differential equation in \mathbf{R}^4 that has the rotational symmetries

$$(x_1, x_2, x_3, x_4) \rightarrow (x_1 \cos \varphi - x_2 \sin \varphi, x_1 \sin \varphi + x_2 \cos \varphi, x_3, x_4),$$

a representation of $\mathbf{SO}(2)$. The unit sphere \mathbf{S}^3 is flow-invariant under the new equation and attracts every trajectory with non-zero initial condition. Let f_0 be the vector field defined in \mathbf{S}^3 by the new equations. There are two equilibria given by:

$$\mathbf{v} = (0, 0, 0, +1) \quad \text{and} \quad \mathbf{w} = (0, 0, 0, -1)$$

that, under the conditions on α_1, α_2 above, are saddle-foci of different Morse indices. They share a two-dimensional invariant manifold, $W^s(\mathbf{v}) = W^u(\mathbf{w})$, the two-sphere $\mathbf{S}^3 \cap \{x_3 = 0\}$ that lies in the fixed-point subspace of the symmetry $\tilde{\kappa}_2(x_1, x_2, x_3, x_4) = (x_1, x_2, -x_3, x_4)$ inherited from κ_2 . There is also a pair of one-dimensional connections $[\mathbf{v} \rightarrow \mathbf{w}]$ in the plane of points fixed by the rotational symmetry. Since $\dot{\theta}$ is positive near \mathbf{v} and negative near \mathbf{w} , the two saddle-foci have different chirality. The vector field f_0 satisfies properties (P1), (P2) and (P4).

The third and final step is to obtain property (P3). This implies breaking the rotational symmetry. The vector fields $f_\lambda = f_0 + \lambda g$ do not have the two-dimensional connection for generic g and for small values of λ . Let g be a vector field in \mathbf{R}^4 tangent to \mathbf{S}^3 , that does not have the symmetry $\tilde{\kappa}$ nor all the rotational symmetries $\mathbf{SO}(2)$, but for which $\tilde{\kappa}_1(x_1, x_2, x_3, x_4) = (-x_1, -x_2, x_3, x_4)$ is still a symmetry. The last requirement ensures that the one-dimensional connection remains for the perturbed vector field $f_\lambda = f_0 + \lambda g$, maintaining the other properties. An example of the result of this construction is equation (6.14) below.

Our results are illustrated with numerical simulations, which have been obtained using the dynamical systems package *Dstool*.

6.2 The example

Our example is the one-parameter family $f_\lambda(X)$ of vector fields on $\mathbf{S}^3 \subset \mathbf{R}^4$, defined by the differential equation in \mathbf{R}^4 :

$$\begin{cases} \dot{x}_1 = x_1(1 - r^2) - x_4x_2 - \alpha_1x_1x_4 + \alpha_2x_1x_4^2 \\ \dot{x}_2 = x_2(1 - r^2) + x_4x_1 - \alpha_1x_2x_4 + \alpha_2x_2x_4^2 \\ \dot{x}_3 = x_3(1 - r^2) + \alpha_1x_3x_4 + \alpha_2x_3x_4^2 + \lambda x_1x_2x_4 \\ \dot{x}_4 = x_4(1 - r^2) - \alpha_1(x_3^2 - x_1^2 - x_2^2) - \alpha_2x_4(x_1^2 + x_2^2 + x_3^2) - \lambda x_1x_2x_3 \end{cases} \quad (6.14)$$

where $r^2 = x_1^2 + x_2^2 + x_3^2 + x_4^2$ and $\alpha_2 < 0 < \alpha_1$ with $\alpha_1 + \alpha_2 > 0$.

The unit sphere \mathbf{S}^3 is invariant under the flow of (6.14) and every trajectory with nonzero initial condition is asymptotic to it in forward time, so $f_\lambda(X)$ is a well defined vector field on \mathbf{S}^3 for each λ , with the two equilibria \mathbf{v} and \mathbf{w} . The linearisation of $f_\lambda(X)$ at $(0, 0, 0, \varepsilon)$ with $\varepsilon = \pm 1$ has non-radial eigenvalues

$$\alpha_2 - \varepsilon\alpha_1 \pm i \quad \text{and} \quad \alpha_2 + \varepsilon\alpha_1.$$

Under the conditions above, \mathbf{v} and \mathbf{w} are hyperbolic saddle-foci, \mathbf{v} has one-dimensional unstable manifold and two-dimensional stable manifold; \mathbf{w} has one-dimensional stable manifold and two-dimensional unstable manifold.

For $\lambda = 0$, the one-dimensional invariant manifolds of \mathbf{v} and \mathbf{w} lie in the invariant circle $Fix(\mathbf{SO}(2)) \cap \mathbf{S}^3$ and the two-dimensional invariant manifolds lie in the invariant two-sphere $Fix(\mathbf{Z}_2(\tilde{\kappa}_2)) \cap \mathbf{S}^3$. Thus,

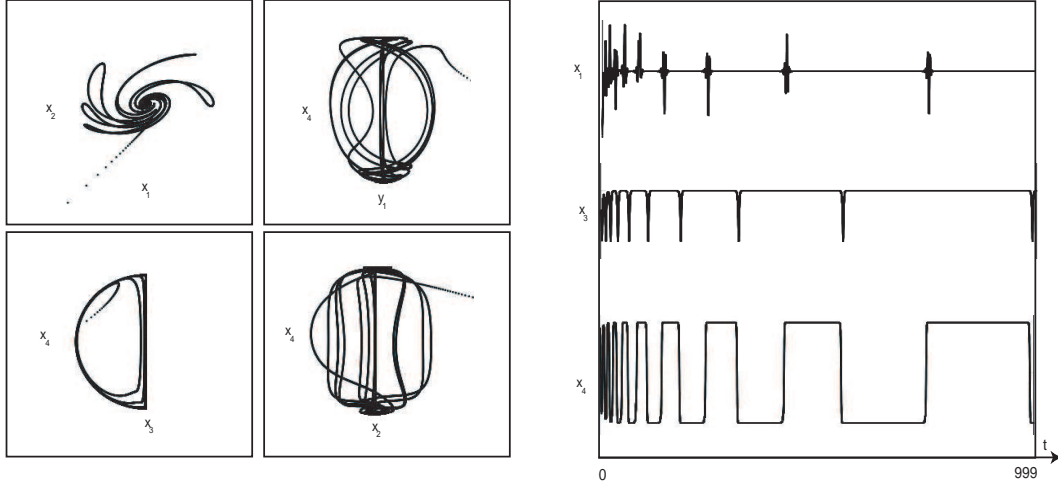


Figure 10: Example of a solution of equation (6.14) for $\lambda = 0$ that accumulates asymptotically on one of the Bykov cycles in the network. Left: Projection in the (x_1, x_2) , (x_1, x_4) , (x_3, x_4) and (x_2, x_4) -planes of the trajectory with initial condition $(-0.5000, -0.1390, -0.8807, 0.3013)$, corresponding to $\alpha_1 = 1$ and $\alpha_2 = -0.1$. Right: Time series for the same trajectory.

symmetry forces the invariant manifolds of \mathbf{v} and \mathbf{w} to be in a very special position: they coincide. The two saddle-foci, together with their invariant manifolds form a heteroclinic network Σ that is asymptotically stable by the criteria of Krupa and Melbourne [25, 26]. Indeed since $\alpha_2 < 0 < \alpha_1$, it follows that $\delta = \frac{C_{\mathbf{v}}}{E_{\mathbf{v}}} \frac{C_{\mathbf{w}}}{E_{\mathbf{w}}} = \left(\frac{\alpha_2 - \alpha_1}{\alpha_2 + \alpha_1} \right)^2 > 1$, where E_X and C_X denote the real parts of the expanding and contracting eigenvalues of $Df_0(X)$ at $X = \mathbf{v}$ and $X = \mathbf{w}$, respectively. The network Σ can be decomposed into two cycles. Due to the symmetry and to the asymptotic stability, trajectories whose initial condition lies outside the invariant fixed point subspaces will approach in positive time one of the cycles. The fixed point hyperplane $\text{Fix}(\mathbf{Z}_2(\tilde{\kappa}_2))$ prevents random visits to the two cycles; a trajectory that approaches one of the cycles in Σ . The time-series of Figure 10 shows the increasing intervals of time spent near the equilibria. The sojourn time in any neighbourhood of one of the saddle-foci increases geometrically with ratio δ .

The parameter λ should control the transversality of the 2-dimensional local invariant manifolds. Care needs to be taken with numerical integration of systems with heteroclinic cycles and networks, because rounding errors may cause qualitatively incorrect results. We have not attempted to prove analytically the transversality – we defer this analysis to a future paper. The switching mechanism described in [2, 4] operating in our network ensures that most trajectories will visit most parts of a neighbourhood of the network, as suggested in Figure 11.

6.3 Different chirality

The example given here in (6.14) is similar to that reported in [40]. The latter has been constructed using the standard lift technique and thus the equation for the angular coordinate θ in the plane $(x_1, x_2, 0, 0)$ is $\dot{\theta} = 1$. Since this plane is perpendicular to the plane where the connection $[\mathbf{v} \rightarrow \mathbf{w}]$ lies, trajectories must turn around the connection in the same direction and the nodes have the same chirality. In the case of example (6.14), the chirality at the two saddle-foci is different, also by construction: since $\dot{\theta} = x$, near \mathbf{v} we have $\dot{\theta} > 0$ and near \mathbf{w} we have $\dot{\theta} < 0$. Chirality does not have any impact on the asymptotic stability of the network, making our work completely consistent with the Krupa and Melbourne criterion [25, 26]. In the simulations presented here we have used the same parameters and initial conditions reported in [40], to facilitate the comparison of the two cases.

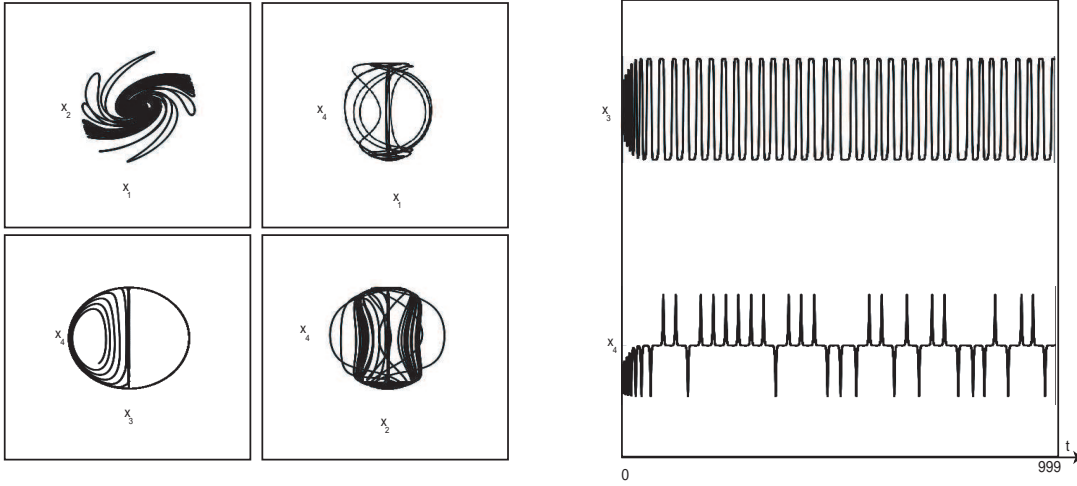


Figure 11: Example of a solution of equation (6.14) for $\lambda = 0.05$ that visits the two primary Bykov cycles in the network. If the two-dimensional manifolds $W^s(\mathbf{v})$ and $W^u(\mathbf{w})$ first meet transversely (which is generically the case), then there are trajectories doing these visits in any prescribed order in a behaviour called switching. Left: Projection in the (x_1, x_2) , (x_1, x_4) , (x_3, x_4) and (x_2, x_4) -planes of the trajectory with initial condition $(-0.5000, -0.1390, -0.8807, 0.3013)$, corresponding to $\alpha_1 = 1$ and $\alpha_2 = -0.1$. Right: Time series for the same trajectory.

References

- [1] M.A.D. Aguiar, S.B.S.D. Castro, *Chaotic switching in a two-person game*, Physica D, 239, 1598–1609, 2010
- [2] M.A.D. Aguiar, S.B.S.D. Castro, I. S. Labouriau, *Dynamics near a heteroclinic network*, Nonlinearity, 18, 391–414, 2005
- [3] M.A.D. Aguiar, S.B.S.D. Castro, I. S. Labouriau, *Simple Vector Fields with Complex Behaviour*, Int. Jour. of Bifurcation and Chaos, Vol. 16, 2, 369–381, 2006
- [4] M.A.D. Aguiar, I.S. Labouriau, A.A.P. Rodrigues, *Switching near a heteroclinic network of rotating nodes*, Dynamical Systems: an International Journal, Vol. 25(1), 75–95, 2010
- [5] A. Arneodo, P. Couillet, C. Tresser, *Possible new strange attractors with spiral structure*, Comm. Math. Phys. 79, 573–579, 1981
- [6] P. Ashwin, P. Chossat, *Attractors for Robust Heteroclinic Cycles with Continua of Connections*, J. Nonlinear Sci., Vol. 8, 103–129, 1998
- [7] R. Bowen, *A horseshoe with positive measure*, Invent. Math. 29, 203–204, 1975
- [8] R. Bowen, *Equilibrium States and the Ergodic Theory of Anosov Diffeomorphisms*, Lect. Notes in Math, 1975
- [9] V.V. Bykov, *Orbit Structure in a Neighbourhood of a Separatrix Cycle Containing Two Saddle-Foci*, Amer. Math. Soc. Transl, Vol. 200, 87–97, 2000
- [10] P. Channell, G. Cymbalyuk, A. Shilnikov, *Origin of Bursting through Homoclinic Spike Adding in a Neuron Model*, Physical Review Letters, PRL 98, 134101–134105, 2007
- [11] F. Dumortier, S. Ibañez, H. Kokubu, *Cocoon bifurcation in three-dimensional reversible vector fields*, Nonlinearity 19, 305–328, 2006

- [12] M. Field, *Lectures on bifurcations, dynamics and symmetry*, Pitman Research Notes in Mathematics Series, Vol. 356, Longman, 1996
- [13] P. Glendinning, C. Sparrow, *T-points: A codimension Two Heteroclinic Bifurcation*, J. Stat. Phys., 43, No. 3–4, 479–488, 1986
- [14] M.I. Golubitsky, I. Stewart, D.G. Schaeffer, *Singularities and Groups in Bifurcation Theory*, Vol. II, Springer, 2000
- [15] N.K. Gavrilov, L.P. Shilnikov, *On three-dimensional dynamical systems close to systems with a structurally unstable homoclinic curve*, Part I, Math. USSR, Sbornik 17, 467–485, 1972
- [16] S.V. Gonchenko, M.C. Li, *On hyperbolic dynamics of multidimensional systems with homoclinic tangencies of arbitrary orders*, preprint, 2011
- [17] S. V. Gonchenko, L.P. Shilnikov, D.V. Turaev, *Dynamical phenomena in systems with structurally unstable Poincare homoclinic orbit*, Chaos 6(1), 15–31, 1996
- [18] S.V. Gonchenko, L.P. Shilnikov, D.V. Turaev, *Homoclinic tangencies of arbitrarily high orders in conservative and dissipative two-dimensional maps*, Nonlinearity 20, 241–275, 2007
- [19] J. Guckenheimer, P. Holmes, *Nonlinear Oscillations, Dynamical Systems and Bifurcations of Vector Fields*, Springer-Verlag, 1983
- [20] J. Guckenheimer, P. Holmes, *Structurally stable heteroclinic cycles*, Math. Proc. Camb. Phil. Soc, 103, 189–192, 1988
- [21] P. Holmes, *A strange family of three-dimensional vector fields near a degenerate singularity*, J. Diff. Eqns, 37, 382–403, 1980
- [22] A.J. Homburg, B. Sandstede, *Homoclinic and Heteroclinic Bifurcations in Vector Fields*, Handbook of Dynamical Systems, Vol. 3, North Holland, Amsterdam, 379–524, 2010
- [23] A. Katok, *Lyapunov exponents, entropy and periodic orbits for diffeomorphisms*, IHES Publ. Math., Vol. 51, 137–173, 1980
- [24] V. Kirk, A.M. Rucklidge, *The effect of symmetry breaking on the dynamics near a structurally stable heteroclinic cycle between equilibria and a periodic orbit*, Dynamical Systems: An International Journal, Vol. 23(1), 41–83, 2008
- [25] M. Krupa, I. Melbourne, *Asymptotic Stability of Heteroclinic Cycles in Systems with Symmetry*, Ergodic Theory and Dynam. Sys., Vol. 15, 121–147, 1995
- [26] M. Krupa, I. Melbourne, *Asymptotic Stability of Heteroclinic Cycles in Systems with Symmetry, II*, Proc. Roy. Soc. Edinburgh, 134A, 1177–1197, 2004
- [27] I.S. Labouriau, A.A.P. Rodrigues, *Global Generic Dynamics Close to Symmetry*, Journal of Differential Equations, Vol. 253, 8 2527–2557, 2012
- [28] I.S. Labouriau, A.A.P. Rodrigues, *Partial Symmetry Breaking and Heteroclinic Tangencies*, in S. Ibáñez, J.S. Pérez del Río, A. Pumariño and J.A. Rodríguez (Eds), Progress and challenges in dynamical systems, Proceedings in Mathematics and Statistics; Springer-Verlag, 281–299, 2013
- [29] J. Lamb, O. Stenkin, *Newhouse regions for reversible systems with infinitely many stable, unstable and elliptic periodic orbits*, Nonlinearity, 17, 1217–1244, 2004
- [30] I. Melbourne, *Intermittency as a codimension three phenomenon*, J. Dyn. Stab. Syst., 1, 347–367, 1989
- [31] I. Melbourne, M.R.E. Proctor, A.M. Rucklidge, *A heteroclinic model of geodynamo reversals and excursions*, In: P. Chossat, D. Armbruster, I. Oprea (Eds), Dynamo and dynamics, A mathematical challenge. Dordrecht: Kluwer, 2363–370, 2001

- [32] L. Mora, M. Viana, *Abundance of strange attractors*, Acta Math. 171, 1–71, 1993
- [33] S.E. Newhouse, *Diffeomorphisms with infinitely many sinks*, Topology, 13, 9–18, 1974
- [34] S.E. Newhouse, *The abundance of Wild Hyperbolic Sets and Non-Smooth Stable Sets for Diffeomorphisms*, Publ. Math. Inst. Hautes Études Sci., Vol. 50, 101–151, 1979
- [35] I.M. Ovsyannikov, L.P. Shilnikov, *On systems with saddle-focus homoclinic curve*, Math. USSR Sbornik, 58, 557–574, 1987
- [36] A. Palacios, H. Juarez, *Cryptography with Cycling Chaos*, Physics Letters A, Vol. 303, 5-6, 345–351, 2002
- [37] J. Palis, F. Takens, *Hyperbolicity and sensitive chaotic dynamics at homoclinic bifurcations*, Cambridge University Press, 1993
- [38] A.A.P. Rodrigues, *Persistent switching near a heteroclinic model for the geodynamo problem*, Chaos, Solitons & Fractals, 47, 73–86, 2013
- [39] A.A.P. Rodrigues, *Repelling dynamics near a Bykov cycle*, Journal of Dynamics and Differential Equations, Vol. 25 (3), 605–625, 2013
- [40] A.A.P. Rodrigues, I.S. Labouriau, *Spiralling dynamics near heteroclinic networks*, Physica D: Non-linear Phenomena, 268, 34–49, 2014
- [41] A.A.P. Rodrigues, I.S. Labouriau, M.A.D. Aguiar, *Chaotic Double Cycling*, Dynamical Systems: an International Journal, Vol. 26(2), 199–233, 2011
- [42] V.S. Samovol, *Linearization of a system of differential equations in the neighbourhood of a singular point*, Sov. Math. Dokl, Vol. 13, 1255–1959, 1972
- [43] L.P. Shilnikov, *A case of the existence of a countable number of periodic motions*, Sov. Math. Dokl., 6, 163–166, 1965
- [44] L.P. Shilnikov, *On a Poincaré–Birkhoff problem*, Math. USSR Sb. 74(3), 353–371, 1967
- [45] D. Turaev, L.P. Shilnikov, *An example of a wild strange attractor*, Math. USSR Sb. 189 (2), 353–371, 1967
- [46] L. Wen, *Homoclinic tangencies and dominated splittings*, Nonlinearity 15, 1445–1469, 2002
- [47] J.A. Yorke, K.T. Alligood, *Period-Doubling Cascade of Attractors: A prerequisite for Horseshoes*, Communications in Mathematical Physics, 101, 305–321, 1985